First steps into the Unknown: Potential field surveying as an affective first step in exploration - A Uno fault example South Australia, Australia

Thesis submitted in accordance with the requirements of the University of Adelaide for an Honours Degree in Geophysics

[Matthew Mark Musolino]

November 2015

THE UNIVERSITY of ADELAIDE

TITLE : [FIRST STEPS INTO THE UNKNOWN: POTENTIAL FIELD SURVEYING AS AN AFFECTIVE FIRST STEP IN EXPLORATION - A UNO FAULT EXAMPLE SOUTH AUSTRALIA, AUSTRALIA]

RUNNING TITLE

Potential field surveying – Uno Fault

ABSTRACT

The Uno Province in South Australia is a current focus of mineral exploration. The province, is bounded to the north by the Gawler Range Volcanics, a large felsic igneous province of mesoproterozoic age that overlies the palaeproerozoic basement. The nature of the boundary is postulated to be structurally controlled by the east-west trending Uno fault. However, little is known of the morphology of the fault. The fault, over time, has been continually extrapolated eastward with minimal geological rational. Information and knowledge adhering to the nature of the fault, its possible extent and the exact boundaries between geological units adjacent to it, does not yet exist. To provide new constraints on the Fault, two lines of gravity data were procured in June 2015. The lines were approximate 52 km and 27 km long, and comprised 156 stations spaced approximately 250 m to 1 km apart. It's hoped that description of the planning phases and the two transect lines of variable gravity station spacing produced a valuable replicable method for this line of work. Regional elevations changes are small (less than 150m) so that only simple gravity reductions methods were applied and the data were tied into a reference South Australian gravity framework. The lines were designed to cross the boundary of the GRV approximately at right angles, although stations had to be collected along roads for logistical reasons. Two-dimensional modelling of the fault using representative densities for the major lithological units shows that the Uno Fault represented a clear boundary in physical properties, but the data could not determine fault from unconformity. The continuation of the fault was not detected to the east in the Siam line. Anomalous areas other than the fault were investigated and discussed including parts of the Hutchinson's group and the geometry of the Hiltaba suite. Conclusions were bounded by the uncertainties inherent in non-unique solutions. However possible explanations to gravitational trends along both lines have been stated and may aid in the continued exploration of this area for minerals.

KEYWORDS
Potential Field
Gravity Surveying
Gravity Technique
Uno Fault
2d Modelling
Gawler Volcanic Ranges

TABLE OF CONTENTS

List of Figures and Tables

1. INTRODUCTION

The Uno fault is believed to be a structural boundary along the south of the Lower Gawler Range Volcanics a 1592+/-3Ma year old felsic igneous province covering in excess of 500km^3 north of the town of Kimba (Figure 1) (Turner 1970; Johns & Solomon 1953; Thomson 1970; Allen et al. 2008). The area is of significant economic importance and exploration is currently underway proximal to the fault (Investigator Resources Limited 2014; Whitten 1963). Most information gathered about the fault was in 1970 by Turner who suggested dip directions, extent, geological structures and hypothesised links to mineralisation. However little was confirmed about the nature of the boundaries between the GRV and the underlying units (being a fault or unconformity) as well as the throw and extent of the fault.

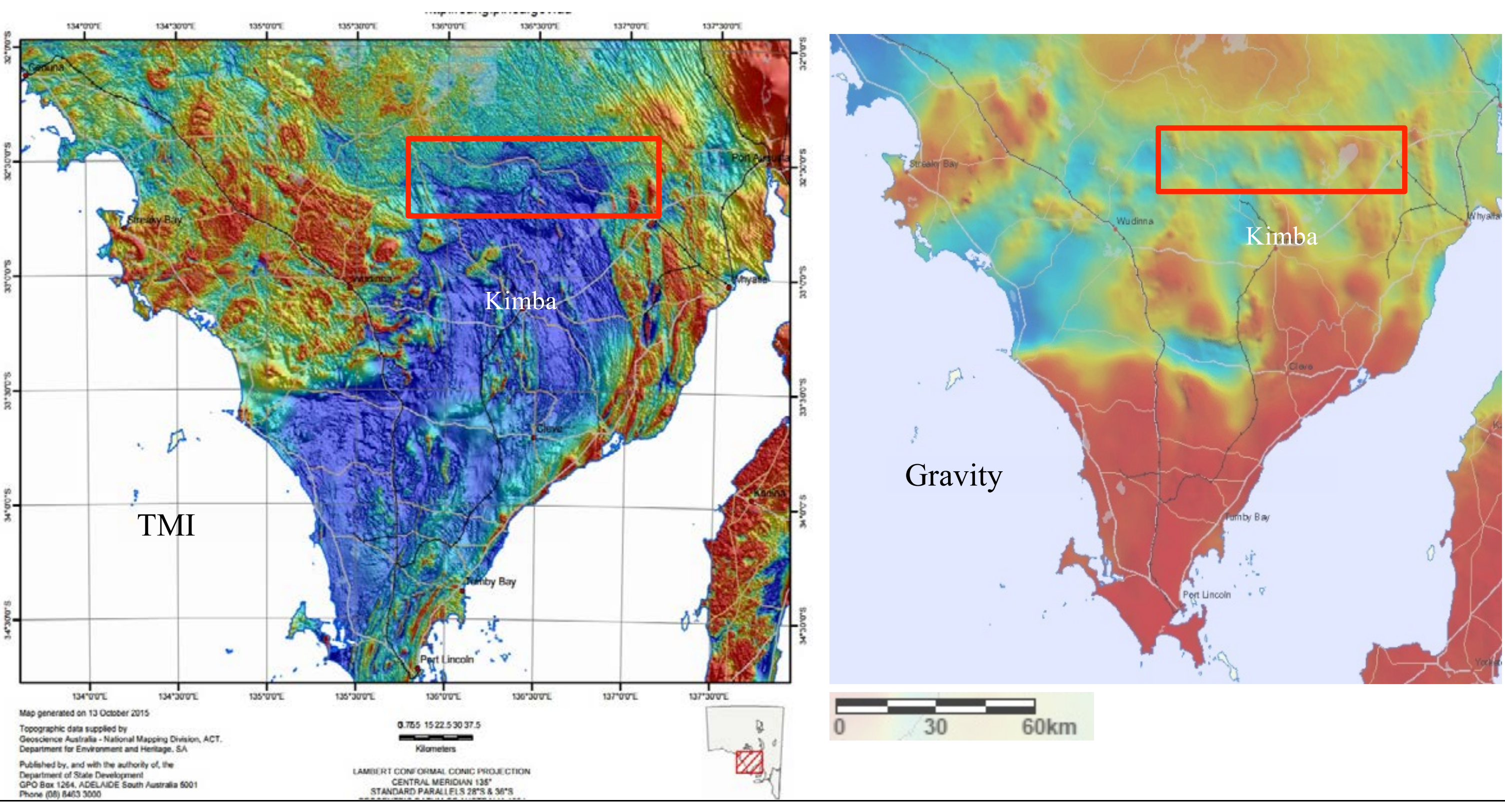

Figure 1. LEFT TMI image of the Peninsula. The area boxed is where the GRV bounds the older southern units and covers the basement magnetic trends. This boundary is the suspected location of the Uno fault. There is a noticeable north to south magnetic response change. The lateral extent of the boundary from the magnetics is approx. 100km W-E. RIGHT state gravity grid shows a response but resolution is too low detect the fault.

Gravity surveys have shown to be successful in detecting hydrothermal alteration, fault nature, and mineral anomalies (Locke & Ronde 1987; Johnson and Fujita 1985; Grauch 1988) Data obtained from these types of surveys have been useful in determining stress fields and possible deposit shape (Xu et al. 2015; Yong 1994; Sibson & Scott 1998) However due to the nature of the method it's possible that factors including metamorphic grade, low density gradients and burial can be detrimental to accurate assessment. (Irvine & Smith 1990)

The goal of the study is to achieve a better understanding the nature of the Uno Fault and developing an effective gravity survey method. The method is to be both efficient and economically viable. It's believed that by collecting gravity data it'll be possible to discern structural boundaries and nature of the formations in the province. Additionally the project strives to discover whether or not gravity data and 2d modelling is sufficient in linking mineralisation and the fault.

The current state gravity grid shows major structural bounds but is too low in base station density to discern complex or smaller features. To remedy this
Two N-S gravity surveys stretching 52km and 27km with differential spacing have been conducted north of Kimba. 2d models were produced from 103 and 43 points of base station data. This data, along with other geophysical data i.e. state grid magnetics, is hoped to accurately describe fault nature. The aim of investigating links to mineralisation will come from looking at potential routs of fluid flow and detecting if hydrothermal alteration is present, while also determining structural geology through geophysical modelling. Furthermore looking at known ore deposits in the area and if their ore body shapes are a reflection of fault stress will aid in linking mineralisation and the fault. The method itself (utilisation of both land based gravity and other regional magnetic data) will also be assessed in terms of efficiency and possibility for continued application.

Worldwide, industry's thirst for metals increase daily and it's important that efficient techniques for mineral exploration continue to be developed and/or practiced. It's hoped that the research methods as well as outcome will be beneficial to exploration of fault related mineralisation worldwide.

2. GEOLOGICAL SETTING/BACKGROUND

2.1 Study Area

The study area is located 490km north west of Adelaide South Australia, Australia and deep inland of the Eyre Peninsular

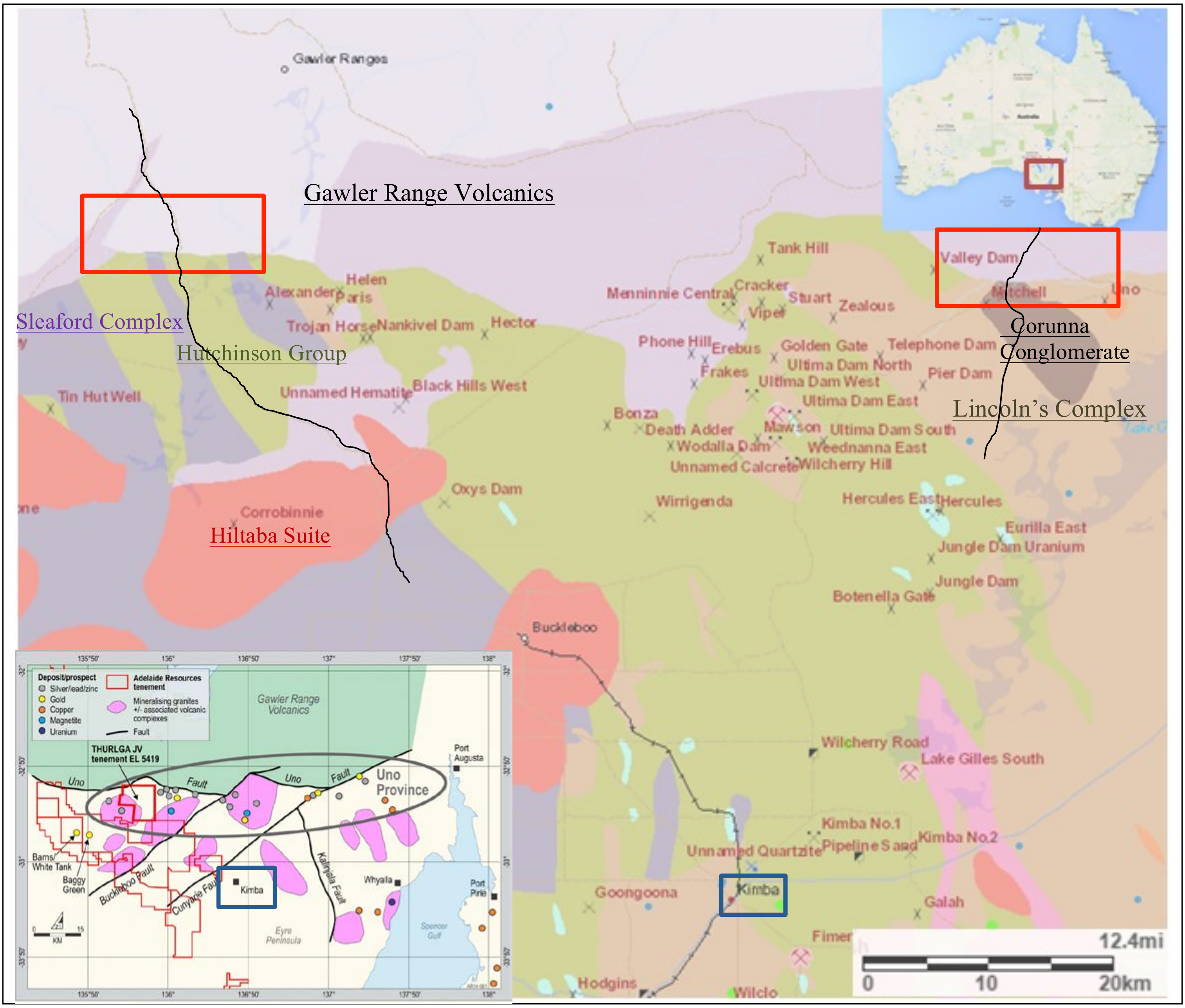

Figure 2. Top right shows a Google Map image showing relative location of Adelaide, Kimba and Buckleboo station. Bottom Left depicts the inferred location of the fault to the mineralised areas (adapted from IRL 2014). Centre, shows the survey area and geological formations therein, as reference, Kimba can be seen bottom centre. North west is the Buckleboo line and to the north east is the Siam or 'Uno' line. Coloured dots indicate earthquake epicentres (Blue being lower magnitude and green higher) Names in red refer to discovered mineral deposits. The Uno 'fault' is boxed in red and the two black lines depict the roads the data points were taken. SARIG 2015

2.2 Gawler Volcanic Ranges

The Uno Fault is believed to band the southern boundary of the Gawler Range Volcanics (GRV) South Australia, Australia. The GRV have been extensively studied and the literature describes the area sufficiently. Allen et al. (2008) simply state that the area is a large interpolate igneous province that formed during mesoproterzoic supercontinent assembly. They continue by describing its dominant felsic units and short eruption timing of the volcanic events. Magma sources are suspected to be from partial melting of the lower crust beneath the semi-stable continental platform neighbouring the developing Adelaide Geosyncline. The magmas that formed the GRV were injected to the upper crust where the enrichment of volatiles promoted immense ash flow eruptions.

Two areas have been separated and defined as the upper and low zones of the GRV (Blissett et al.1993). The lower zone which is of interest in this study consists of felsic lava domes with relatively moderate spreading of felsic lavas. Ignimbrites and scattered andesitic cone volcanoes are also present. The lower volcanic zone itself is divided into two main exposures the, Chitanilga Volcanic Complexes and Glyde Hill Volcanic Complexes. The basement Chitanilga basaltic layer hosts above minors of andesites and rhyolites. The Glyde Hill Complex is composed of felsic units that have been intruded by mineralising dykes (Blissett et al. 1993). Investigator Resources Limited (IRL) (2014) has suggested mineralising dykes are present in the Paris deposit and have a metal source of approximately 40km in depth. Both Allen et al. (2008) and Investigator Resources Limited (2014) suggest that the area shows traits of a mega caldera.

2.3 Uno fault

Turner described the Uno Fault as a normal dip slip fault formed as a result of differential subsidence in the north, and limited by south-east trending dykes as described above and by Johns & Solomon (1953). The inferred extent of the fault has been changed over time however there is little to no surface expression (Thomson 1970).Dip angle of the fault is suggested to be very steep and northward, although no specifics are given. (Turner 1970).SARIG's (2015) database suggests the fault timing is Archean to Early Mesoproterzoic. Results of Turners (1970) lab work on porphyroclasts and ribbons of quartz in the brecciated, flinty, quartz filled, fine grained igneous rocks proximal to the fault showed evidence that the local geology was subject to increased vertical movement rather than lateral movement. Geological and isotopic analysis determined that the rocks adjacent to the fault were not formed in-situ (Compston et al. 1966).

Economic mineral deposits formed by hydrothermal fluids close to the fault have been discussed and are currently being investigated (Figure 2 bottom left) (Investigator Resources Limited 2014; Whitten 1963)

2.4 Geological units

Referring to figure 2, The Sleaford complex (seen in aqua) comprises banded metabasalts and sediments as well as synorogenic intrusives these are visible in the Carnot Gniesses. The Dutton Suite within the Sleaford Complex houses granites and granodirites.These have undergone low grade metamorphism (Daly & Fanning 1993). The famous Mesoproterzoic Hiltaba Suite Granites (seen in red) have intruded into this Sleaford Complex. In the north, the suite is covered by the Gawler Range Volcanics (see in in light purple). The Sleaford Complex is then overlain by the Hutchins group (seen in olive green) (Vassallo & Wilson 2001). This complex sits between the two transects.

Several magmatic suites seen to the east collectively known as the Lincoln's Complex (seen in brown) intruded into the Hutchins group as well. (Parker 1993)
The west line, north of Buckleboo runs through the Hiltaba Suite Granites, The Sleaford Complex, The Hutchinson Group and the GRV. The east line goes through the Paleoproterzoic 'Lincoln Complex' Gneisses , Mesoproterzoic Corunna Conglomerate and the lower GRV (SARIG 2015).

Table 1. Ages and densities of rock units in the survey area. Data from SARIG (2015) petrophysical database

*Densities approximated

Name	Age (Ma)	Mean Density (gcm^{-3})
Sleaford Complex	2479+/-9Ma - 2430+/-6Ma	2.80*
Hutchinson Group	~1730-1692Ma	2.75

Lincolns Group	1731+/-7Ma (Middle Camp Granite); ~1715Ma (Paxton Granite)	2.74
Hiltaba Suite	1613+/-19 - 1575+/-7Ma	2.68
Gawler Range Volcanics	1592+/-3Ma	2.65
Corunna Conglomerate	1587+/-15Ma	2.67*

World class deposits such as The Olympic Domain have associations with some of these complexes and general area, highlighting the importance for understanding and investigation. Presence of the Hiltaba Suite granite for example is a large determining factor when deciding on exploration areas (Ferris et al. 2015)

Understanding the geological history as well as the relationships between complexes and the Uno fault will help to better exploration targeting.

2.5 Background: Gravity as an exploratory geophysical method

Gravity is a potential field method of geophysical exploration. The method can locate subsurface anomalies by detecting geological mass changes.

To do that accurately however , factors must be corrected for, these include but are not limited to; latitude, height, tidal changes, Bouguer correction, free air correction, instrument drift, terrain correction, topographic correction and moving platform correction (Dentith & Mudge 2014; Blakely 1996;Vajk 1956)

Gravity surveys have been used in exploration to investigate areas of hydrothermal alteration, possible mineralisation zones as well as fault nature (MacLean & Kranidiotis 1987; Locke & Ronde 1987; Johnson and Fujita 1985;Grauch 1988; Represas et al. 2013).The effectiveness of the survey is based on design as well as physical properties of the surveyed geology such as cover and level of metamorphism (Irvine & Smith 1990). It is also may be possible to determine stress fields and possible orientation of ore hosting bodies by gravity survey using equations outlined by Xu et al. (2015) ,Yong (1994) and Sibson & Scott (1998). The gravity method in context of the project is a good start in exploring the fault due to its non-invasiveness, low cost and ease to perform. The South Australian Government also provides free magnetic data which helps to guide the design of the survey. Ideally a seismic line across the fault would yield higher detailed below ground geology.

Land based gravity surveys are comparatively cheaper than airborne surveys but do lack some airborne advantages as discussed by Bell et al. (1999). However land based surveys have proved to be effective and advantageous on their own (Lamontagne et al. 2011). The efficiency of this survey is also to be analysed. It is so that the wider scientific community can benefit from the study, mimic the surveys methods and further use what's been learnt to be efficient in their own projects.

3. GRAVITY DATA COLLECTION

3.1 Survey planning and rational

Originally the project called for a single line along Buckelboo Road. This was further expanded upon discussion with academics and industry/government professionals to best utilize the opportunity. It was decided that two transects, one to the west and one to the east would give a better indication of the continuation of the fault structure and lithological boundaries. The specific position of the transect lines were restricted to road and land access. A route perpendicular to the lithology's and structures was high priority given the 2D modelling interpretative advantageous outlined by Butler (1995) and Bott (1974). Review of Simmons 1964 methods on geological interpretation from variably spaced gravity surveys showed how excellent correlation with real world geology and modelled data can be achieved. The paper however discussed that some areas of interest were not resolved well enough and this lead to the idea of having 250m spacing in areas of particular interest along the Buckleboo and Siam transects. By having the 1km – 250m spacing technique it was hoped that a large enough area was covered in a reasonable time as well as assuring quality data acquisition.

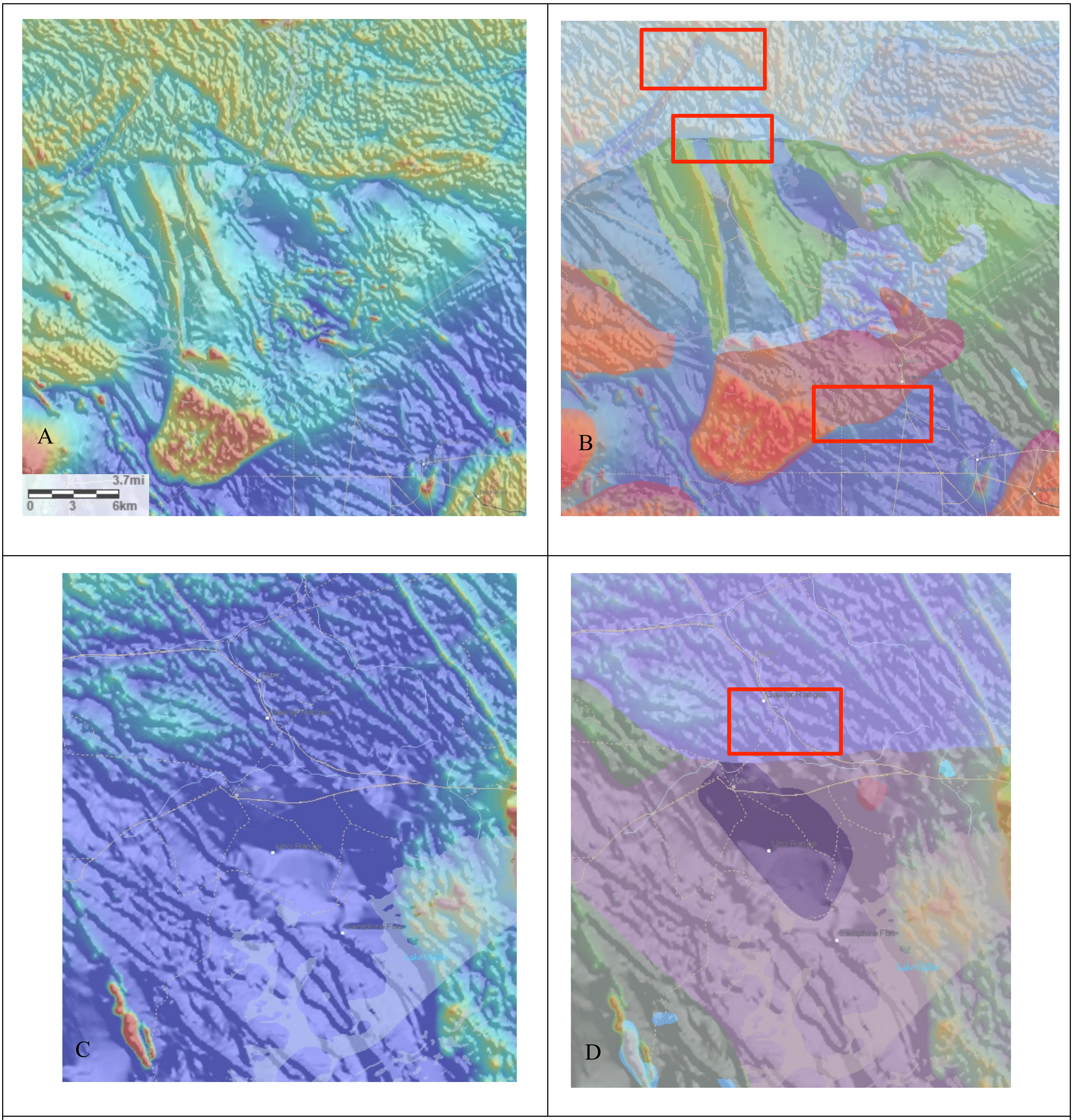

Figure 3. Clockwise starting top left; Geophysical magnetic data of the Buckleboo line, geological overlay of magnetic data of the Buckleboo line as reference, geological overlay of the Siam line as reference, magnetic data of the Siam line. Red boxes show areas of planned infill. SARIG 2015

The South Australia grid of geophysical magnetics data guided the planning for where infill (250m) spacing was to be conducted. Figure 3 shows the magnetics and the geology overlayed for the two lines. Three areas of interest were decided upon due to magnetic features that may represent structure.

The first in the far north is thought to be lower GRV and upper GRV contact but a prominent ridge is observed through the magnetics and it was hoped that the survey may also pick up this structure. The second is the boundary between the Hutchinson Group and the GRV, this is the suggested place of the Uno fault and thus warranted infill. Finally the third is the area between the Hiltaba Suite and the Sleaford Complex that shows a large magnetic change. One area of interest was chosen for the Siam line. A prominent left to right striking magnetic line is seen and although within the GRV is suspected to be an interesting structure to investigate. The fault supposedly runs just below the line however the terrain is inhospitable to travel.

The use of both gravity and magnetics to plan out exploration reflects the work done on combined analysis by Garland (1951)

The investigation and planning lead to two survey transect plans seen in figures (4) and (5)

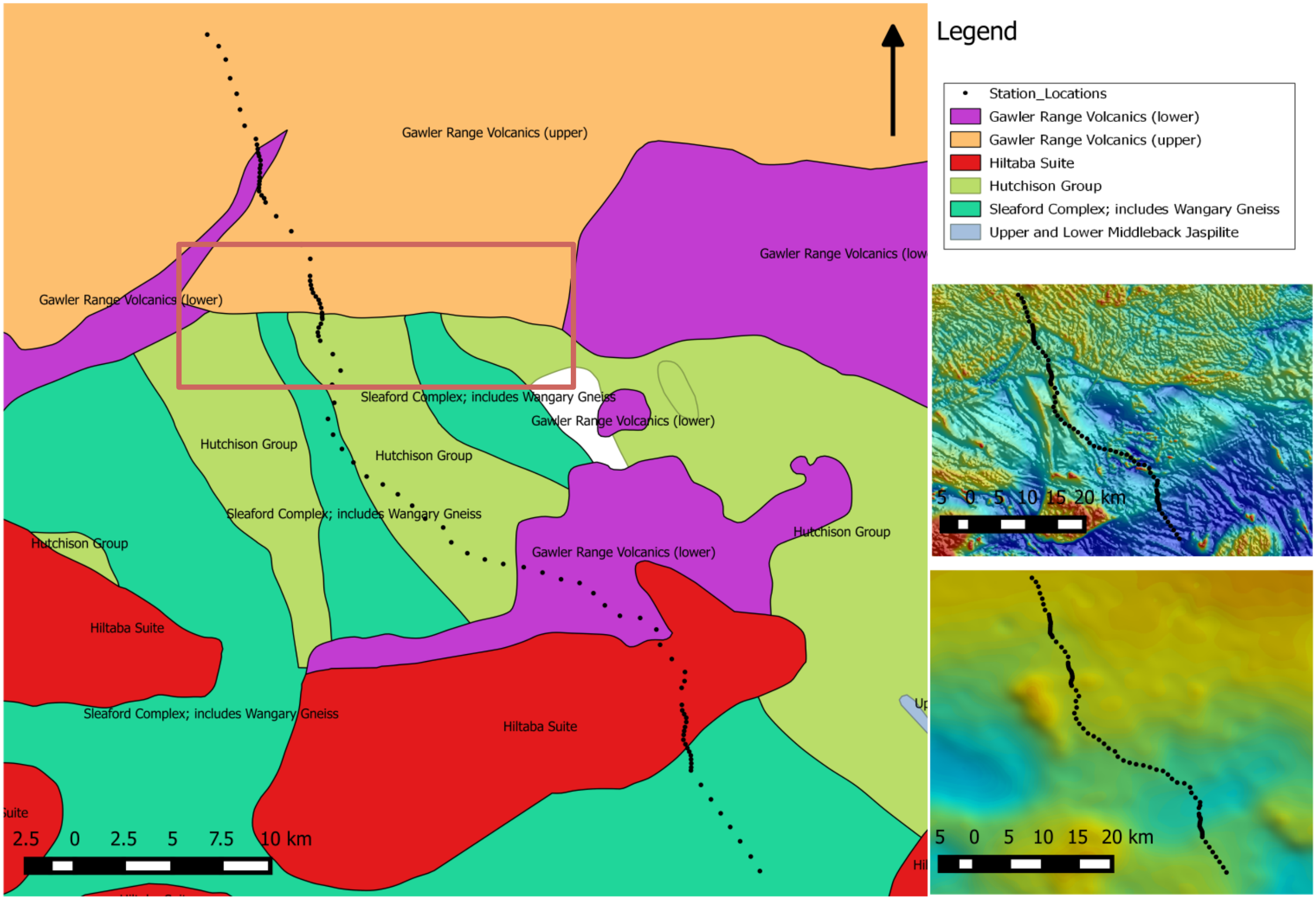

Figure (4) Buckleboo road gravity data station locations mapped across geological units with a red box highlighting the boundary/fault. Density of spacing is 1km with three areas of 250meter infill around areas of interest. The areas of interest can be observed in the top right figure of the magnetics. From south to north, the Hiltaba suite, Sleaford complex boundary the Hutchinson group, UGRV (upper gawler range volcanics) boundary and LGRV, UGRV boundaries. General gravity trend is shown on the bottom right. All figures provided by SARIG adapted by Matthew Musolino 2015

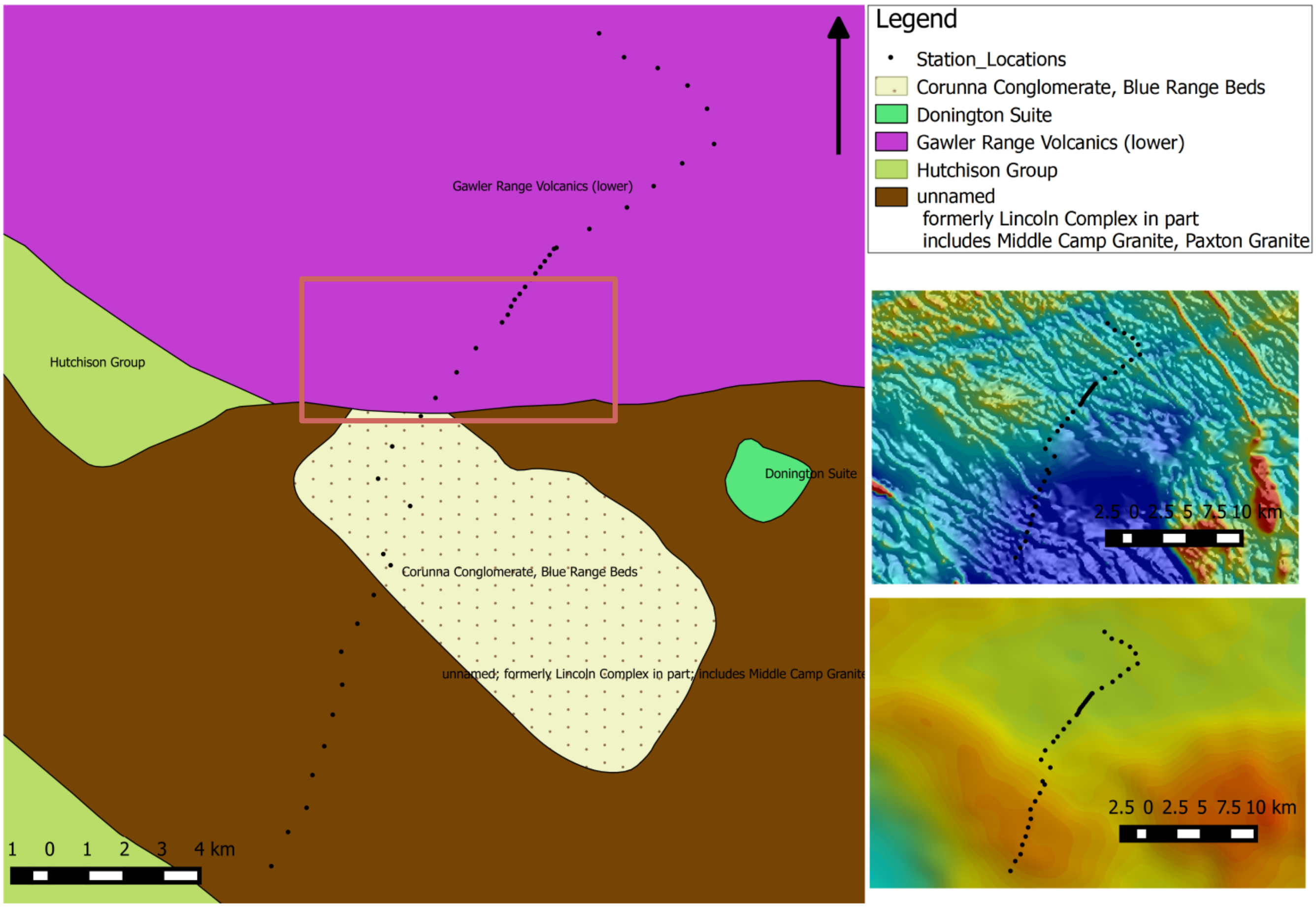

Figure (5) Siam/Uno range gravity data station locations mapped across geological units with the red box highlighting the boundary/fault. Density of spacing is 1km with one area of 250meter infill around an area of interest. The area of interest is due to a prominent structure visible in the magnetics (top left). The gravity trend is shown in the bottom right. All figures provided by SARIG adapted by Matthew Musolino 2015

3.2 Gravity Surveying

Two gravity survey transect routes were selected in collaboration with the South Australian Department of Development and University of Adelaide that were conducted between the 8th and 12th of June 2015. Using Kimba as a base the survey design used was an alternate spacing loop system.

The survey lines were made north south through Buckleboo station and Siam station, South Australia. Two Sokkia GRX1 differential GPS were set up to gather elevation data for both locations at least 6 hours prior to starting the survey. After the new UTC day, data was uploaded to AUSPOS and then used to set up the GPS to take data points and accurate elevation readings. All work was done with a Scintrex CG5 gravity meter and Kimba's absolute gravity marker served as the base station as per Morelli (1976).

A tripod station was set up at a topographic high in the middle of the transect to give the most coverage for the GPS system. Motor vehicles carrying the roving unit and gravity meter were then used to traverse the line in one direction taking measurements each kilometre (or 250m) until contact between the roving GPS and base station was lost, navigation was done using ARCGIS 9 on a Getac laptop.

The position of each reading was marked using a Hand Held GPS – TopCon FC-2500 and hand written time was taken. The base station remained in place and the same activity was conducted in the other direction until connection was lost. The Station was then moved up or down the transverse and the method was repeated. This was the case for both transects.

4. GRAVITY DATA (RESULTS)

4.1 Field processing & corrections

Data was uploaded from the CG5 gravity meter to a computer where it was imported to a Microsoft Excel spread sheet. A series of standard corrections that utilised the loop method (Bouguer, free air, instrument drift etc) were applied to the data using a premade Microsoft excel spread sheet (the specific equations behind the spread sheets are available upon request or as by Denith & Mudge (2014) to give a Bouguer gravity anomaly. Note that tide corrections are inbuilt to the machine and that moving platform or topographic corrections were not applied due to the nature of the survey.

4.2 Gravity observations and results

The northern most part of the Buckleboo line (figure 7) shows a generally more negative gravitational response southward for about 15000m. At this point, a noticeable, sharp 2 mgal change occurs. After this, the response becomes increasingly positive until it drops around 1.8mgal from 19500 onwards. The infill zone at 8000-1000m showed interesting 2mgal movements that were anomalous. The infill zone from 15000 - 19000m also showed an unsmooth trend.

The middle of the Buckleboo line shows a fairly gradual decline southward with observable 4mgal difference between 31000m and 34000m. At 35000m a sharp negative 2.5mgal shift occurs.

The south of the Buckleboo line (figure 7) shows a large 6 mgal difference between 40000 and 45000m. At either side of these lengths the response levels out.

Gravity response over the Siam line (figure 6) became more negative heading northwards, this change happened quite gradually although data collected at 10000m and 15000m shows a mgal response considerably more negative than the points south of them. North of these points however, the response is consistent.

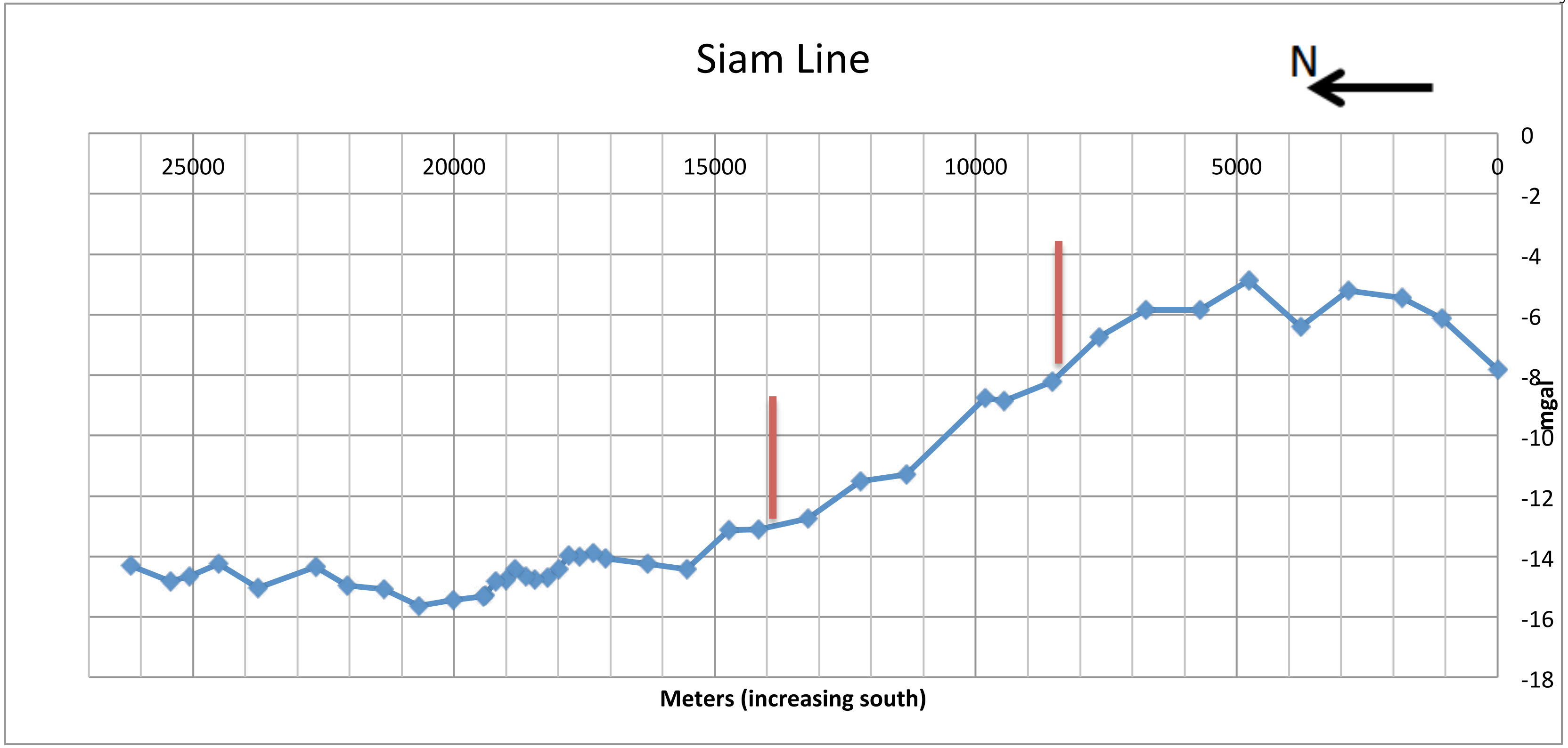

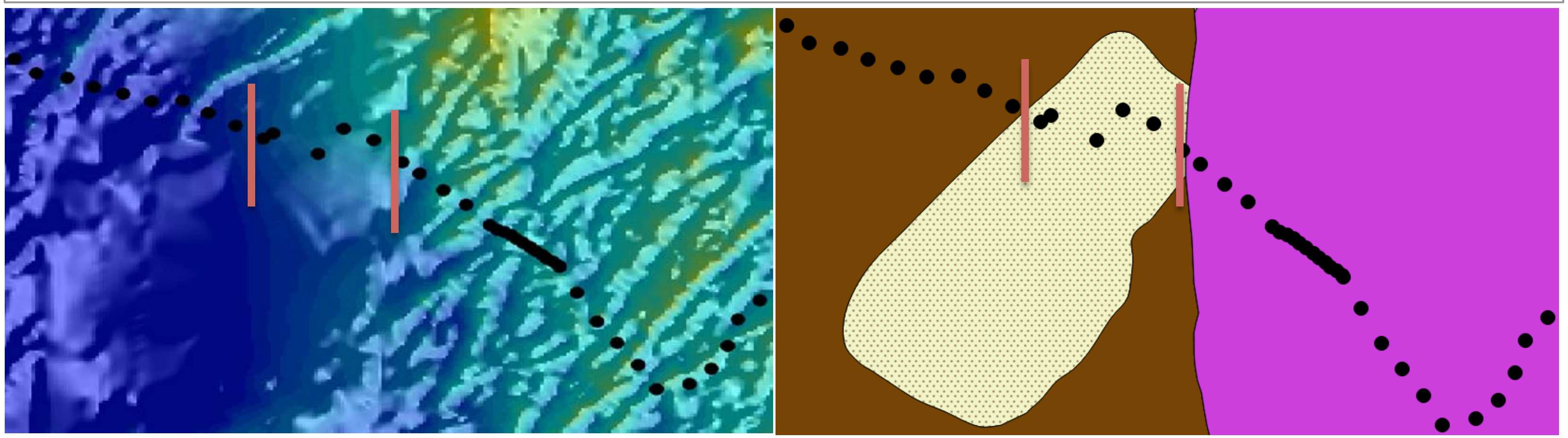

Figure 6 - Gravity response over the Siam line became more negative heading northwards. Change is gradual apart from data collected at 10000m and 15000m. These locations show a mgal response considerably more negative than the points proceeding them. North of these points however, the response is consistent. The red lines denote boundaries and their corresponding gravity readings

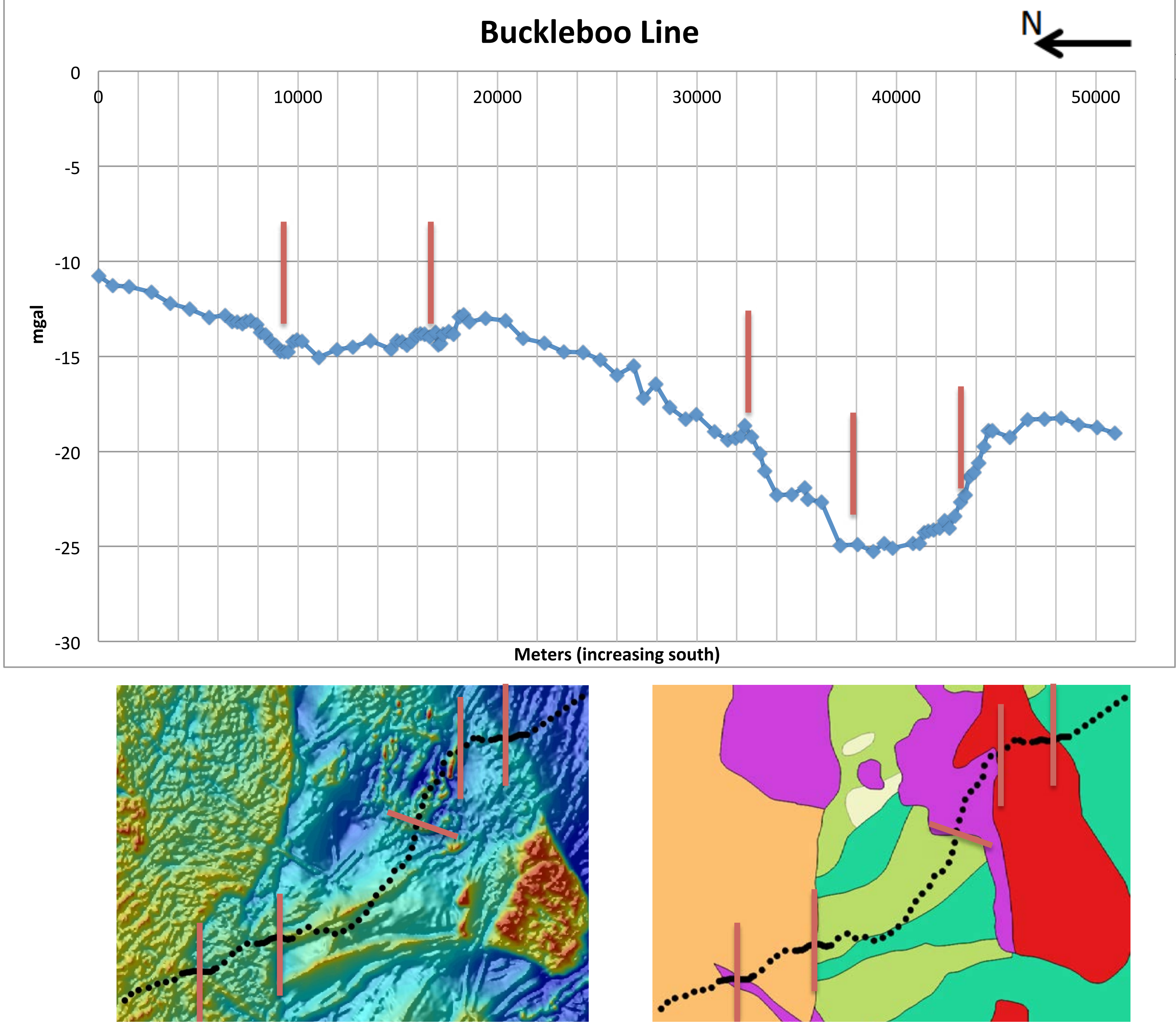

Figure 7

Buckleboo line gravity profile in mgal. A generally more negative gravitational response southward. At 15000m a noticeable, sharp 2mgal change occurs. The response becomes generally most positive after this before dropping 1.8mgal from 19500m onwards .A general negative mgal response heading southward continues (left to right). Anomalous 4mgal differences at 31000m and 34000m are observed as well as sharp negative response of 2.5mgal at 35000m to 36000m .Southern Buckleboo line gravity profile shows a large 6mgal difference between 40000m and 45000m occurs. Responses either side of these limits level out. Red lines depict boundaries along the black dotted stations.

5. GRAVITY INTERPRETATION

5.1 Modelling Assumptions

The modelling program used was Encom : Model vision. 'Notepad ++' was also required to construct the adequate files for input. All GIS work was done using ARCGIS10 and QGIS 2.8.1. Additional data acquisition i.e. densities, were provided by SARIG.

Splitting the Buckleboo line into three separate lines for modelling as seen in figure (8) was performed so that the 2d model (that assumes no lateral movement) better reflected the path the data was taken. This ensured more accurate boundary placement. Consider a best of fit line from the north to the south. This would have a large disparity between the points where the data was taken and said line, due to the curved nature of the transect.

Topography elevation in the models was not corrected for and a flat surface is assumed. A digital elevation map (DEM) was attempted to be implemented into the model however the affect was minimal due to the reasonable flatness of the terrain and was incompatible with many of the modelling features.

Many of the units extend to extensive depths (Vassallo & Wilson 2001; Fraser et al 2010) leading to the assumption that the gravity anomalies were very strongly influenced by the geological units modelled and not cover or deeper units. Surface expressions of multiple units were observed in the field and thus the units are assumed to start at 0 meters in the models.

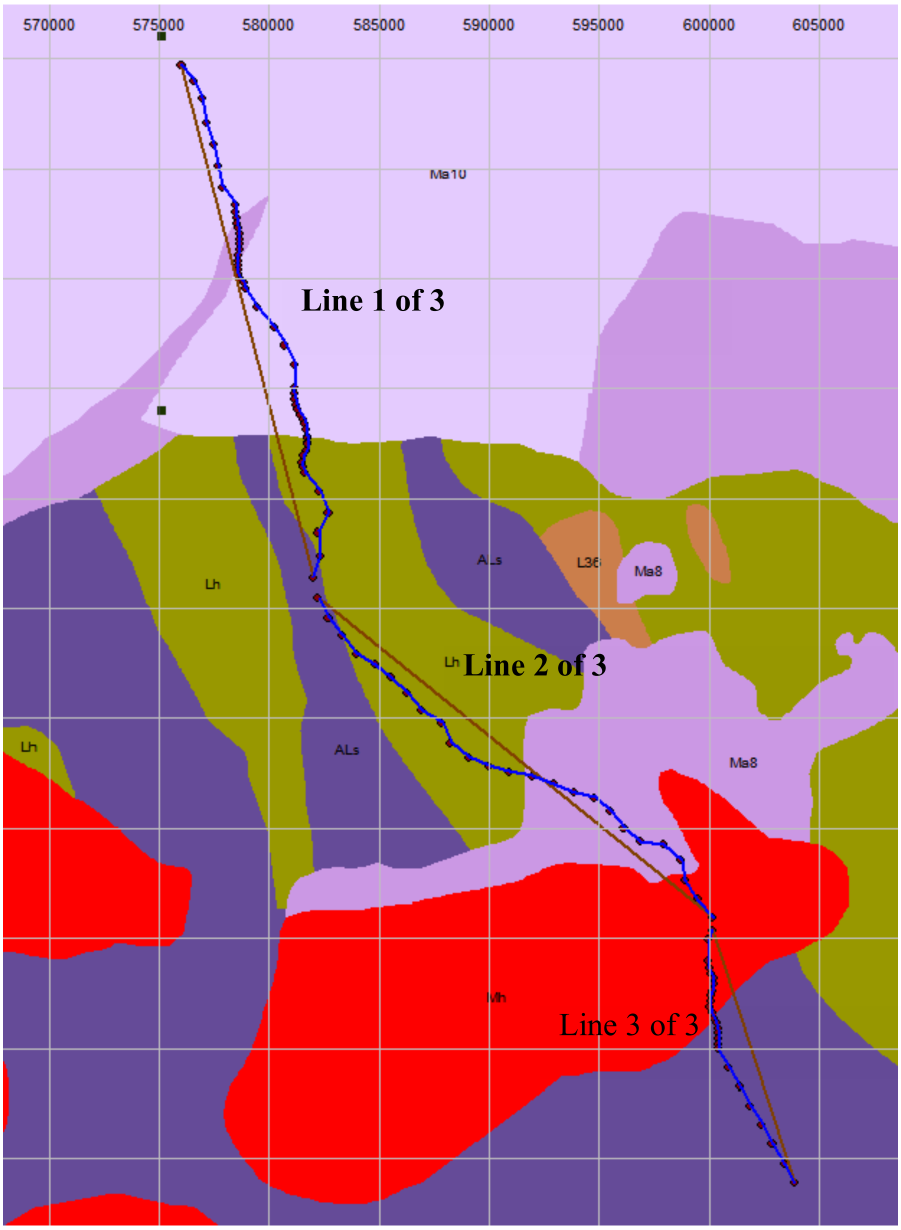

Figure (8) Shown is the Buckleboo line split into three for 2d modelling placed over the geology described previously

A regional was added to the data using the Encom software. The software applied a first order polynomial to the dataset to reveal the regional trend. The technique is described by Beltrao et al. (1991). Adding a regional brought all the data into line with the model and was necessary for accurately fitting the modelled data to the observed.

Densities as previously mentioned were provided by SARIG (2015) each unit was allowed a 0.05g/cm^3 density change during the modelling to best fit the data. A wide spread of the densities for some units in the petrophysical histogram data strengthens the argument for this permission.

Depth extents were lenient. A 2km sway limit was imposed on values from Vassallo & Wilson (2001). Fraser et al (2010) and drill hole data from SARIG (2015)

Dip angles had no constraints since not much is known about the dips of the formations. However throughout the modelling geological plausibility was inherent in the process.

5.2 Modelling techniques

There are many plausible geological mass distributions that can replicate the observed data. Setting tight thresholds around known information (i.e. density) was a start. The boundaries between the geological units were also thought to be very accurate and so the bodies north to south extents were first added. As Bhattacharyya (1978) describes there are two ways to conduct modelling from gravitational data. Forward modelling and inverse modelling, both were utilised in this project.

Forward modelling predicts geophysical data for specific geological structures. The forward method has the benefits of allowing the user to input known data into the model space and work around it (Zhdanov 2002). Inversion is fast, simple to implement and can give a conceptual idea of what the data may reflect underground. The inversion process, although you can set thresholds and parameters, fashions a model purely from the data. It is useful when not much is known about an area (Bhattachayya 1978). Utilisation of both methods helped to create geologically feasible models that also reflected the data sufficiently.

For (figure 9) an inversion was run on the data and a model with the best fit was found, the mathematics behind the inversion of step wise 2D gravity models are described by Nettleton (1942). The inversion morphed the physical properties and geometry of each unit (within set thresholds) and was determined solely from the observed data. This was done for all the lines. Some results were plausible while others were not, so forward modelling was employed to maintain a best fit scenario while still producing geologically plausible models. Forward modelling was aided by the geological information at hand and experience of colleges.

5.3 Modelling results

5.3.1 Buckleboo line

The first model (figure 9) suggests a thin Gawler Range Volcanics that extends 731m in depth. With an average density set at 2.6917 g/cm^3. Continuing south the GRV is bounded by the Hutchinson group and Sleaford complex, the model suggests both dip at

44 degrees northward. Both are modelled down to 5km with a density of 2.7507 g/cm^3 and 2.7856 g/cm^3 respectively. Figure (10) shows the Sleaford group and Hutchinson group at a 90 degree boundary. This is due to them sitting beside each other at this point and it's not a true traverse across each unit. (See figure 8 line 2 of 3) The Hutchinson group dominates this area but there is a section of lower GRV once again extending around 700m.

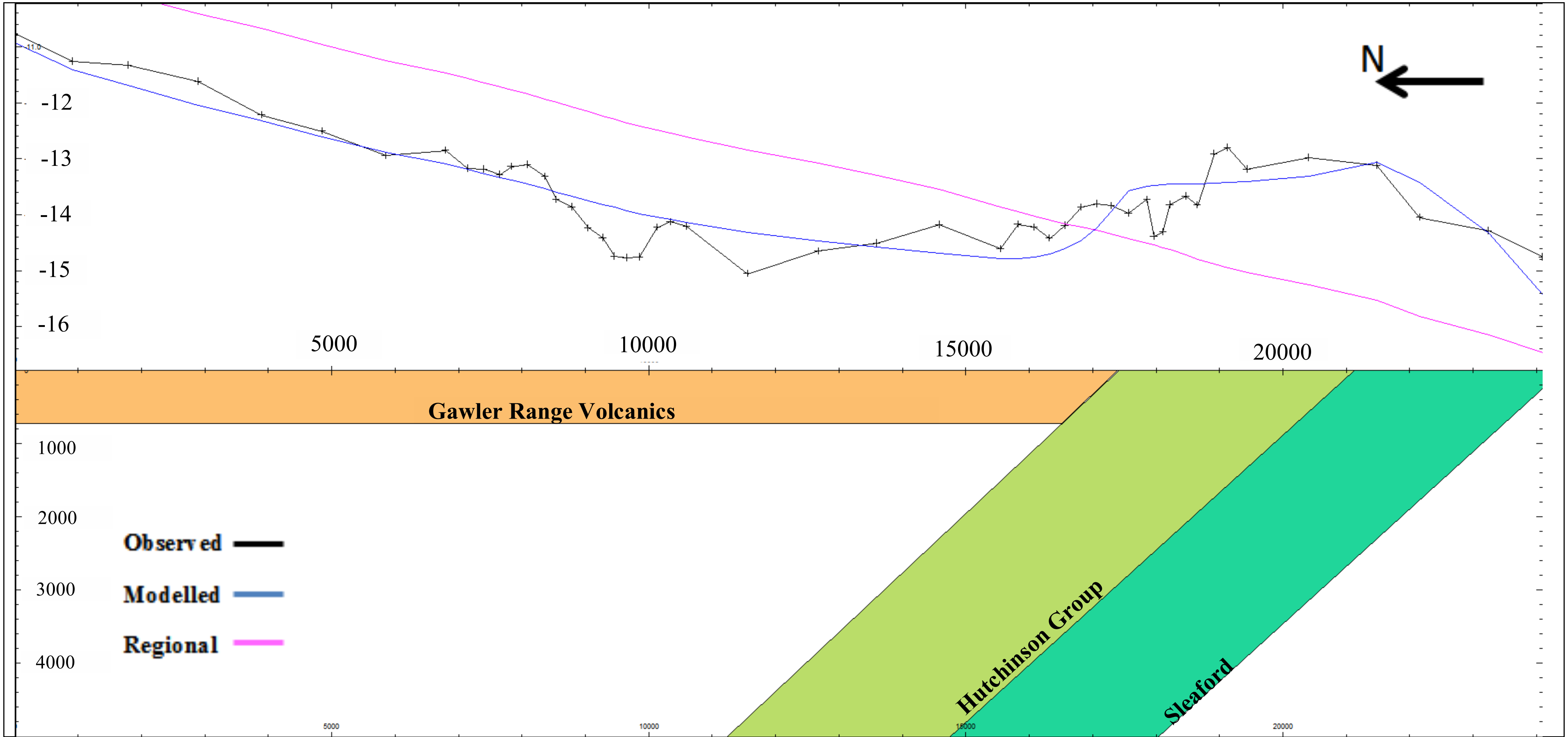

Figure (9) Buckleboo line – Northern End. X axis and lower half of Y axis is length and depth in meters respectively. Upper Y denotes mgal. The black line is the observed gravity data and the blue reflects the gravity profile created by the model. The general trend is a gradual decline southward along the Upper Gawler Range Volcanics (which extend to 750m in depth) however there is a less uniform decline around 7000 meters near the infill, 2 mgal drop is observed .Past 15000m there is a noticeable mgal increase.The model suggests the Sleaford complex and Hutchinson's group dip 41 degrees northwards and extend to approximately 5000m. There are two areas of data infill (250m) in the middle of the UGRV and another at the southern boundary.

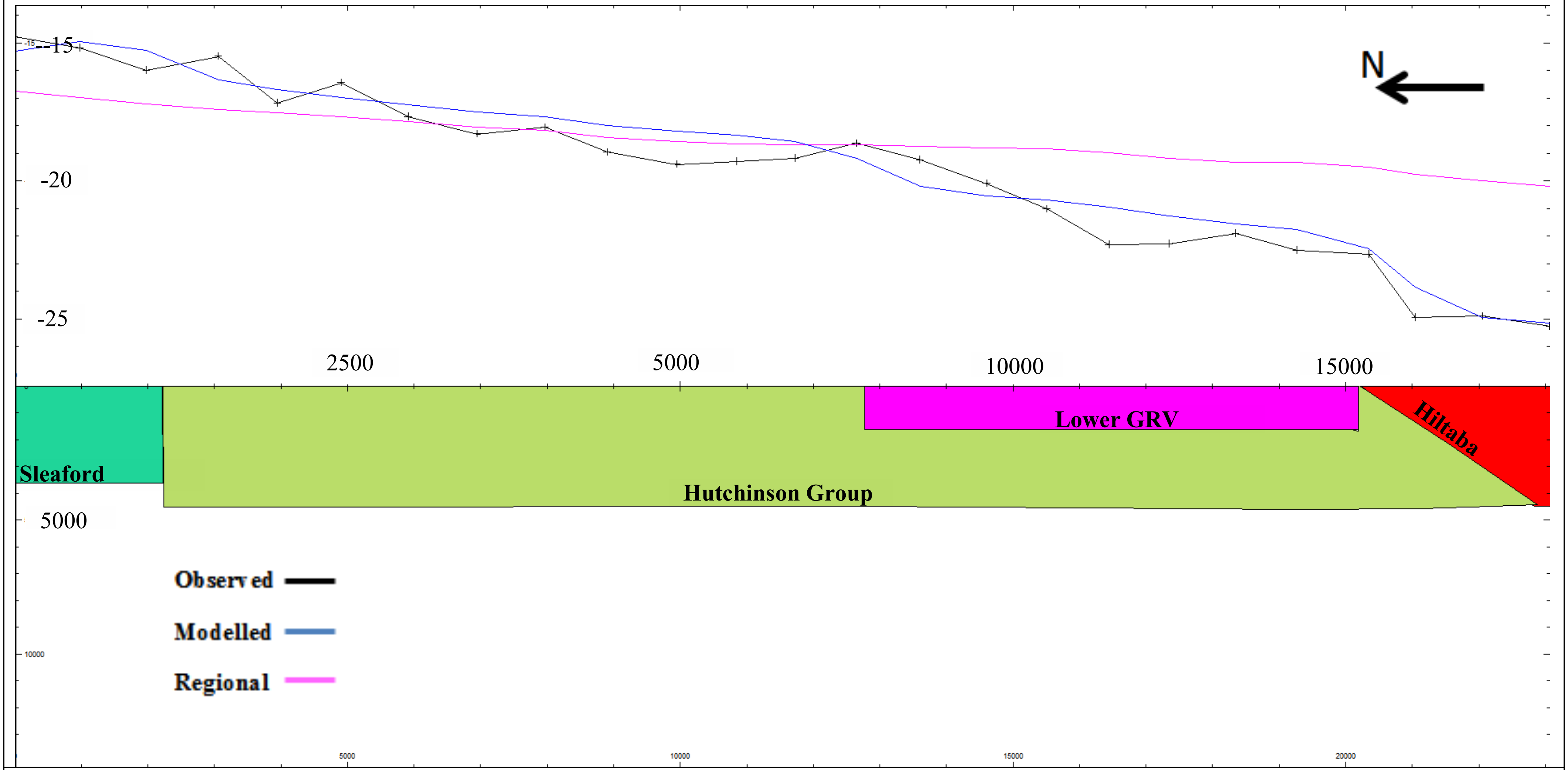

Figure (10) Buckleboo line – Middle section (North to the left of the image) The Hutchinson's group dominates the middle section of the transect and is estimated at 5000m in depth. The overall trend is a decline to the south. A slightly more negative trend is apparent between 12500m and 20000m displaying a 4mgal difference, after this acute 3.5mgal drop is observed at 20500meters.

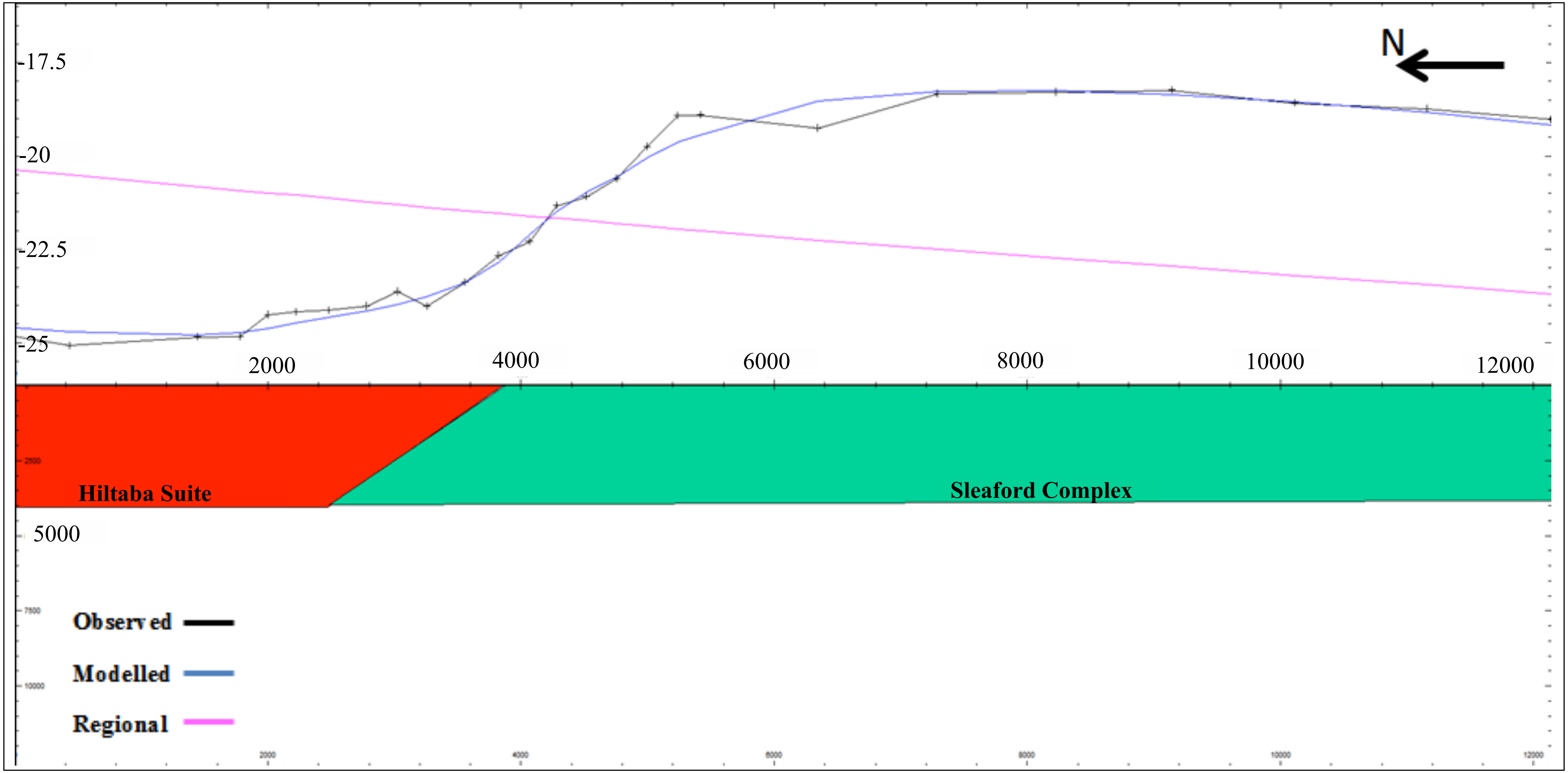
N
-17.5
-20
-22.5
-25
2000
4000
6000
8000
10000
12000
Hiltaba Suite
Sleaford Complex
5000
Observed
Modelled
Regional

Figure (11) Buckleboo line Southern End - The two units in this area extend approximately 4km in depth and the model very accurately follows the observed data. a 7.5mgal difference is observed and the gradient is quite smooth. The higher density of data points (infill) occurs around the boundary between the two groups.

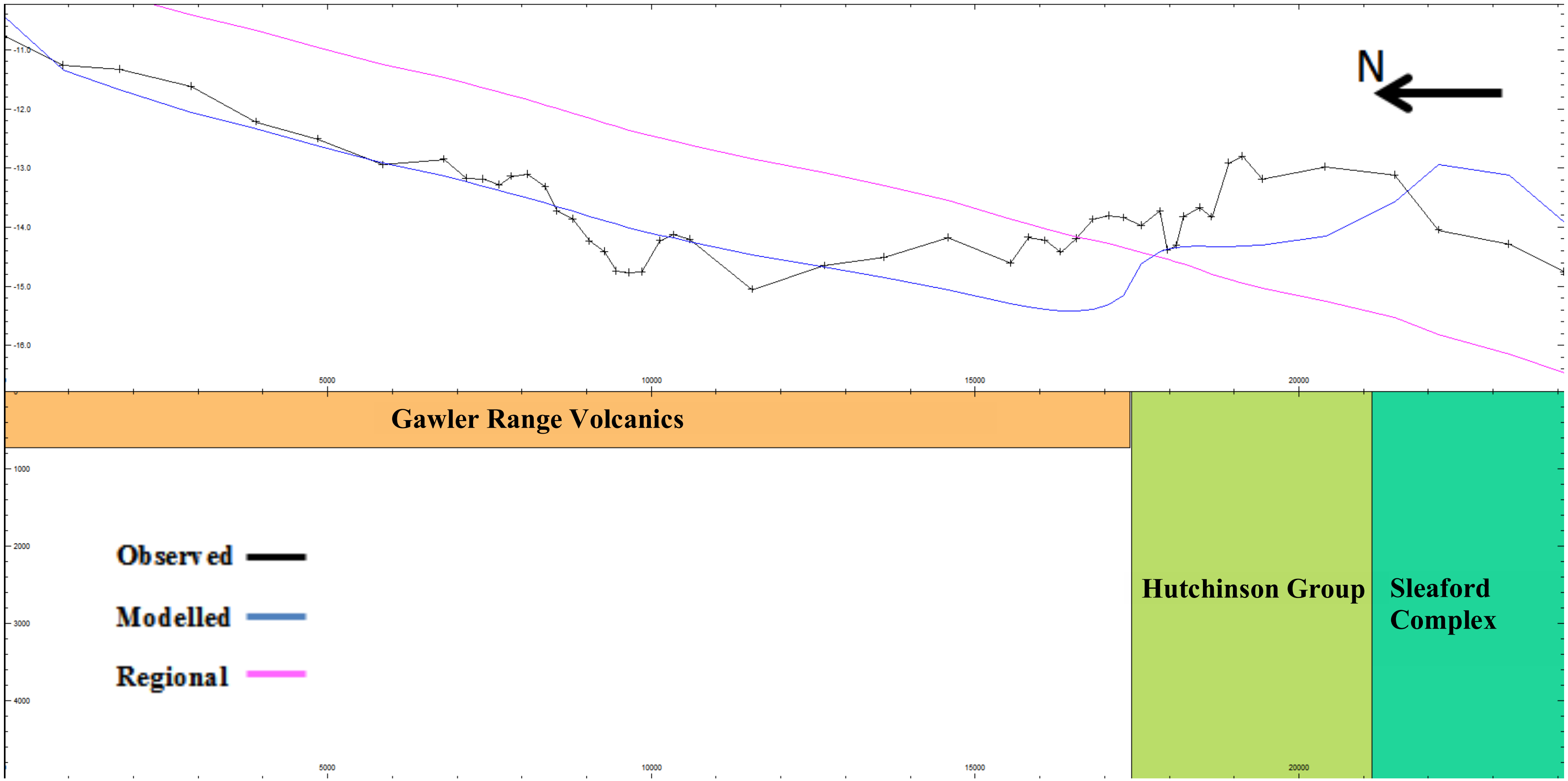

Figure 9.1 Buckleboo line (North) vertical – Vertical tabular blocks have been supplemented instead of those dipping north seen in figure 9. It can be easily visually observed that the modelled data doesn't reflect the observed data as well accurately as the dipping blocks in figure 9.

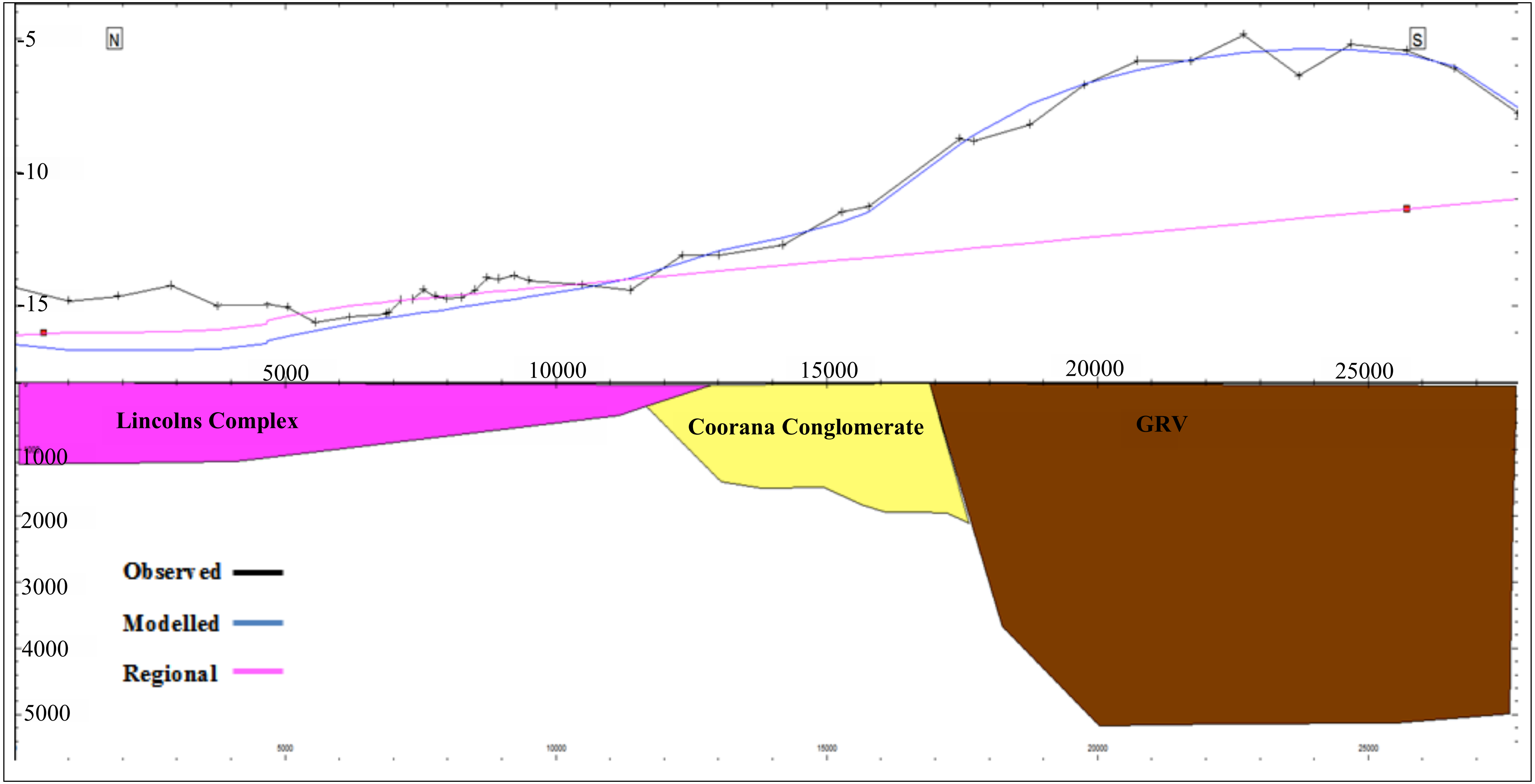
N
S
-5
-10
-15
5000
10000
15000
20000
25000
Lincolns Complex
Coorana Conglomerate
GRV
1000
2000
3000
4000
5000
Observed
Modelled
Regional

Figure (12) Siam line – Full section, North is to the right of the image. An approximate 12mgal gradient occurs as the response decreases to the north and into the lower GRV. The infill of 250m spacing was in the LGRV. The Lincolns group extends 5km while the model predicts the Coorana Conglomerate extending 2.2km (at the deepest and the GRV thickening northward. The modelling predicts a scenario where the GRV flow went over the Conglomerate and stopped (hence the shape) the boundary between the Lincolns and Conglomerate has been moved northward to better fit the model, not much is known about the nature of the boundary.

Interestingly, modelling predicts the best fit scenario requires a southward dip at 34 degrees for the Hiltaba suite. The density for the Hiltaba suite was set at 2.7088 cm/g^3.

At the southern end of the line the Hiltaba contacts the Sleaford. The model best fitted the observed data when a 34 degree northward dip was applied to the structures starting at the 3800m contact. In this area it's thought that the units are slightly thinner (3.5km)

The outcomes from the modelling found that it's possible to fit reasonable geological structures to the gathered observed gravity data along the Buckleboo transect

5.3.2 Siam Line

The models predict the Lincolns complex (model density of 2.72 cm/g^3) extending 5km and the boundary between it and the Coorana Conglomerate (model density of 2.67 cm/g^3)is moved 1.5km northward to better fit the model. The Coorana Conglomerate's root is predicted to be variable as it approaches the GRV (model density of 2.66 cm/g^3). The GRV was modelled to thicken northward from 700m to 1.8km.

6. DISCUSSION

Ambiguity is inherent in gravity modelling and interpretation, this is owing to the non-uniqueness of gravity anomaly solutions. It is to say that many geological models of varying volumes and densities can produce the same gravitational anomaly. (Skeels 1947; Roy 1962) Due to the simplistic 2D modelling and noise levels the inferences on the data have been cautious.

6.1 Buckleboo line

The observed data and modelled data for figure (9) show some large discrepancies between one another. Shown in figure 9.1 are three 90 degree dip tabular structures for reference.
A more complex, dipping geometry like that in figure 9 better conforms to the observed data and is more likely to reflect sub surface structural geology.

The First large discrepancy in figure 9 between observed and modelled data is between 7000m and 10000 meters, it's most likely due to slender arm of LGRV cutting upwards north. The magnetics show a change and so does the base geology (figure 7). The use of gravity has been therefore affective in the accurate detection of small geological changes.

Moving southward along the same line there is the suspected area of the Uno fault. Unfortunately it's not possible to determine the type of fault it is or when the faulting occurred as kinematic information isn't displayed by gravity survey alone. Figure 2 displays epicentres of seismic activity yet the position of the epicentres do not reflect that the fault is currently active. The work by Xu et al. (2015) on modelling stress from gravity data wasn't affective due to the fault activity data needed. It's suggested in order to assume that it's a fault rather than an unconformity surface seismic monitoring would need to be implemented. Field geology information would also be beneficial. Searching for stricken lines in quartz may be able to indicate the in-situ stress fields as well as the possibility of fault fluid flow. Additionally geochemistry work to indicate if any alteration can be detected that may reflect the presence of mineralising fluids similar in nature to those responsible for Olympic dam deposit discussed by Johnson & McCulloch (1995) Or fluorine based fluids discussed by Agangi & McPhie (2010)

The area is prospective for many different types of minerals (Andrews 2013). Not all important information about a landscapes mineral potential comes from positive anomalies.
Although rarer, negative anomalies can indicate local mass loss due to alteration (Lumb 1981) Locke & DeRonde (1987) discuss a 2-4mgal drop in a hydrothermally altered zone within the Golden Cross, New Zealand. Their gravity data and models suggested that the density contrast in their survey found possible sites for gold bearing hydrothermally altered rocks (Figure 13).

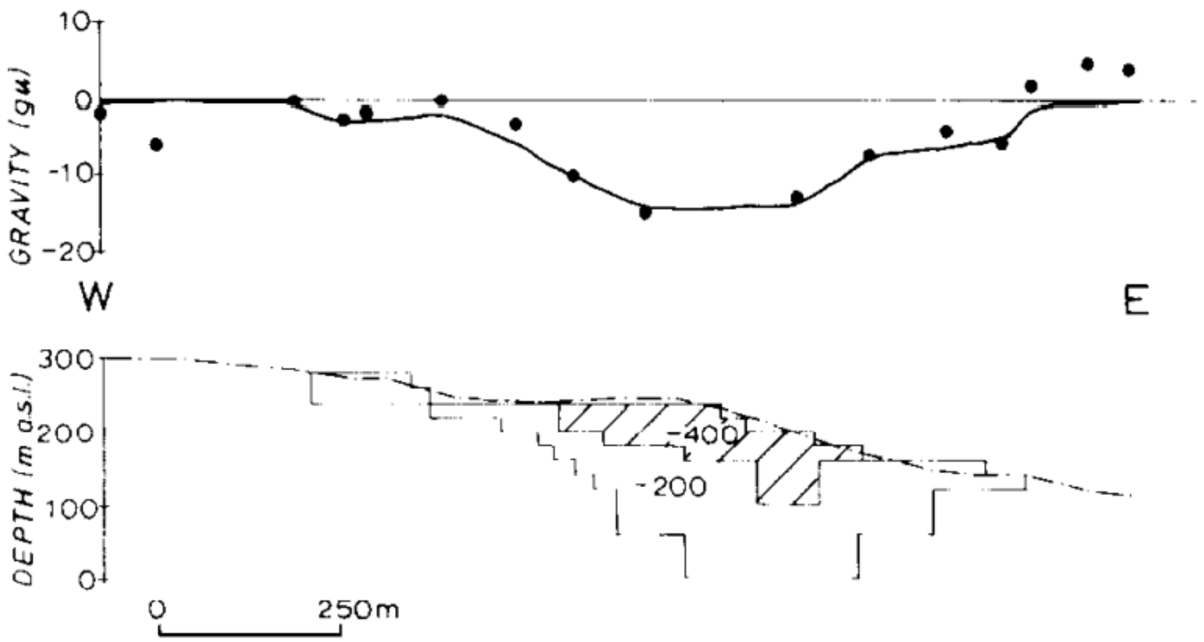

Figure 13 Gravity model, topography, observed residual (dots) and calculated (solid line) gravity anomalies across a hydrothermally altered region 5 km south of Golden Cross. Density contrasts in kg m-'. Locke & DeRonde (1987)

Similarly, studies by Stierman (1984) also concluded chemical alteration in suspected fault zones due to hydrothermal alteration.

It's then reasonable to suggest that the possibility for some of the anomalous negative readings at the edge of the fault (17500-19000m Figure) could possibly be due to hydrothermal alteration.

Likewise in figure 10 the negative gravity anomaly between 3750m and 6250m occurs in what was thought to be a homogenous unit. This area may also warrant further study to see what is producing the mass loss.

Further on down that same line the Hiltaba Suite dips southward, interestingly however in figure 11 the boundary resolves a different dip direction. The geometrical shape is hypothesized to be a magma chamber of post orogenic granites. These granites intruded 1500-1450 Ma (Webb et al. 1986) and the shape predicted by the modelling closely resembles that of a gradual replenishing granitic pluton described by Wiebe & Collins (1998) (Figure 14)

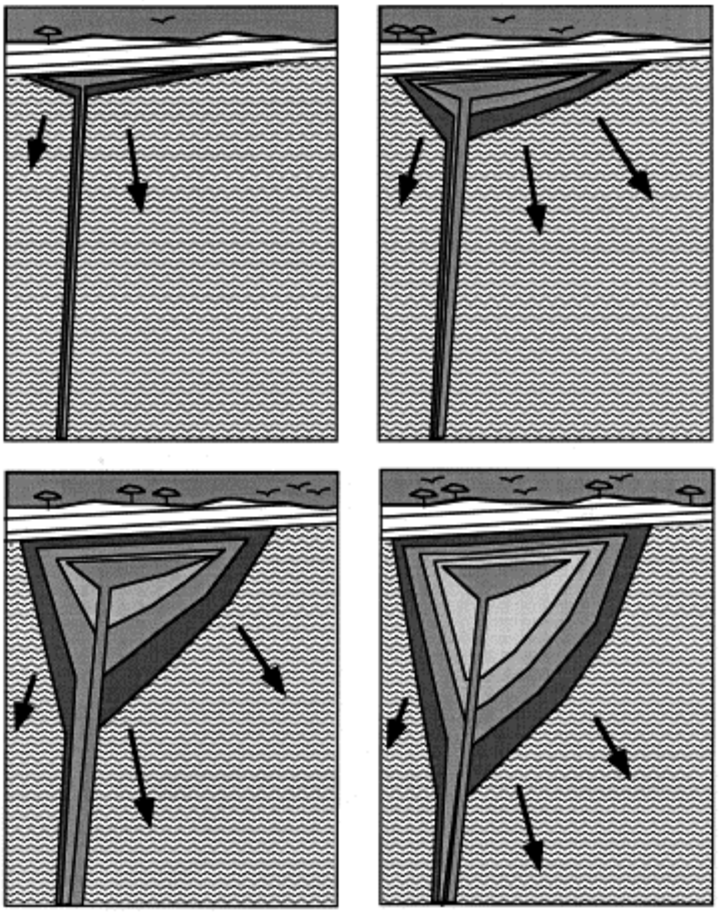

Figure 14 Schematic diagrams showing development of a granitic pluton by gradual replenishment, crystallization, and sinking of the floor and basal cumulates. (Wiebe & Collins 1998)

Additionally the gravity profile of the southern end of the Buckleboo line (figure 11) that shows the Hiltaba suits connection to the Sleaford, closely resembles a model made by Richards & Collins (2004). Their model (figure 15) shows a similar mgal shift of 4-5mgal. The modelled gravity profile at 17.5km-20km has a response like that of the Hiltaba and Sleford boundary. The sharpness of the incline at 19km is steeper however indicating less of a dip.

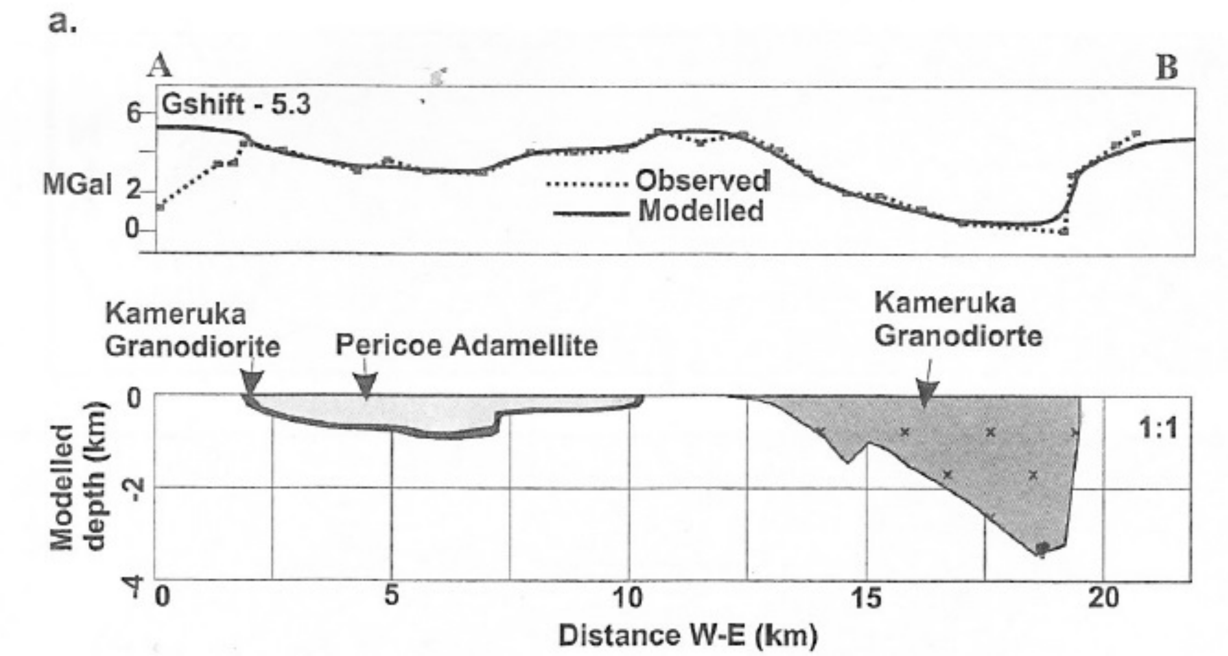

Figure 15 Observed and modelled gravity profiles for the Kameruka granodiorte. (Richards and Collins 2004)

6.2 Siam line

Up to 11000m the model accurately fits the observed data. Further on from this, The GRV's response is shadowed heavily by the regional. Meaning in this area the model response doesn't reflect the observed measurements. However thickening is assumed as that follows the observed data trend when the regional is removed. Furthermore since the original magma flowed southward it's geologically reasonable to suspect an increasing thickness closer to the source.

The Uno fault is not obviously observed in the gravity. In the area of interest there is detection of a boundary but not a fault like response (around 13000m). The infill detects two W-E structures of interest in the magnetics but they are likely to be anomalous subsurface structures and not large scale faults.

A possible reason the fault wasn't detected is that it's suspected to be between the GRV and the older groups south. The transect went across the Coorana Conglomerate, (a younger group) before intersecting one of the older groups (The Lincoln Complex). The fault could have been masked by the presence of this group which has been shown as a possibility inherent in the gravity method (Irvine & Smith 1990). In that case we would then have to assume the faults age is older than that of the Coorana Congolomerate which has a primary age of 1587+/-15Ma (SARIG 2015). Not detecting the fault is in itself important information.

Further study for the Siam line would include another N-S traverse either to the West where there's a Hutchinson's Group boundary directly in contact with the GRV or to the Eat where there is a direct Lincoln's complex boundary.

6.3 Remarks on methodology effectiveness

The collection, processing and analysis of the gravity data has produced reasonable geological models that have revealed a lot about the area not previously known. Furthermore it has created many new questions and hypothesis to investigate.

Data collection was inexpensive and time effective. With the information gathered it's safe to say that the use of gravity as a geophysical exploration method is a great start when looking at an unknown area. The initial time and monetary investment is low, and it paves a path for further exploration techniques.

As for the gravity survey design itself (figure 16) shows that had infill not have been conducted within the zones of interest (shown in blue) many anomalous data points could have been missed, making inferences about the geology less reliable/robust.

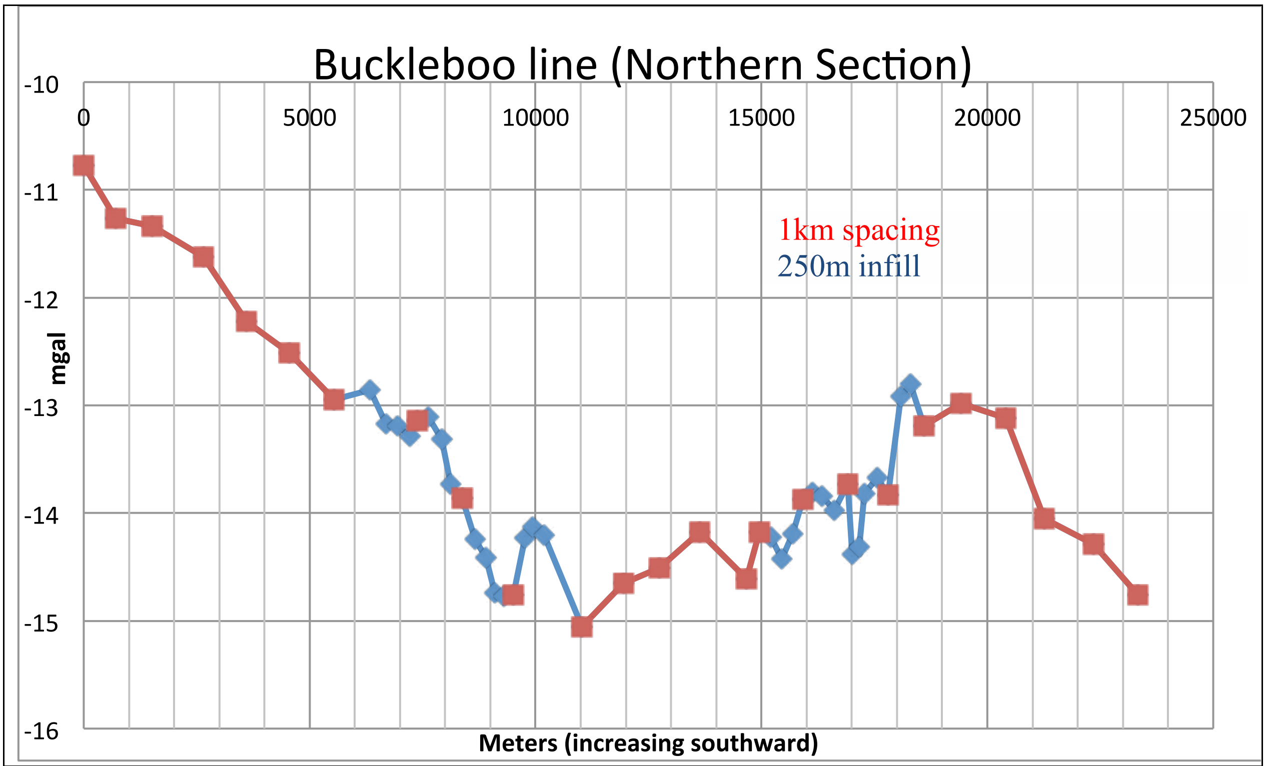

Figure (16) Buckleboo line showing what the data would look like with and without infill

7. CONCLUSIONS

Many core goals of the project have been achieved successfully and those attempted have given insight into how they may be achieved in the future.

- Nature of the fault as well as identifying boundaries of surrounding units were achieved accurately using potential field surveying
- The survey using regional magnetic data and land based gravity was an effective approach into the area due to its ease, low cost and data output.

- Unfortunately stress fields, as well as separation of fault and unconformity were unable to be confirmed purely on the designed survey, however recommendations to discover this have been suggested
- The continuation of the fault between the two transect lines is unconfirmed, the possible reasons for this have been discussed.

In all it's concluded that the survey method and technique used was affective. Potential fields have shown useful in the analysis of faults and related structures. The Uno fault is self (if a fault) has been modelled within the bounds of geological plausibility and the data served as a stepping stone for future mineral and geological exploration the area.

8.ACKNOWLEDGMENTS

Phil Health
Graham Heinson
Matthew Hutchins
Derick Hasterok

9.REFERENCES

AGANGI A., KAMENETSKY V. S. & MCPHIE J. 2010. The role of fluorine in the concentration and transport of lithophile trace elements in felsic magmas: insights from the Gawler Range Volcanics, South Australia. *Chemical Geology* 273, 314-325.

ALLEN S. R., MCPHIE J., FERRIS G. & SIMPSON C. 2008. Evolution and architecture of a large felsic Igneous Province in western Laurentia: The 1.6 Ga Gawler Range Volcanics, South Australia. *Journal of Volcanology and Geothermal Research* 172, 132-147.

ALLEN S., SIMPSON C., MCPHIE J. & DALY S. 2003. Stratigraphy, distribution and geochemistry of widespread felsic volcanic units in the Mesoproterozoic Gawler Range Volcanics, South Australia*. *Australian Journal of Earth Sciences* 50, 97-112.

ANDREWS M. 2013. Investigator's silver lining in South Australia.

BELL R. E., CHILDERS V. A., ARKO R. A., BLANKENSHIP D. D. & BROZENA J. M. 1999. Airborne gravity and precise positioning for geologic applications. *Journal of Geophysical Research: Solid Earth* 104, 15281-15292.

BELTRAO J., SILVA J. & COSTA J. 1991. Robust polynomial fitting method for regional gravity estimation. *Geophysics* 56, 80-89.

BHATTACHARYYA B. 1978. Computer modeling in gravity and magnetic interpretation. *Geophysics* 43, 912-929.

BLAKELY R. J. 1996 Potential theory in gravity and magnetic applications. Cambridge University Press.

BLISSETT A., CREASER R., DALY S., FLINT R. & PARKER A. 1993. Gawler range volcanics. *The Geology of South Australia* 1, 107-124.

BOTT M. H. 1974. The geological interpretation of a gravity survey of the English Lake District and the Vale of Eden. *Journal of the Geological Society* 130, 309-328.

BUTLER D. K. 1995. Generalized gravity gradient analysis for 2-D inversion. *Geophysics* 60, 1018-1028.

COMPSTON W., CRAWFORD A. & BOFINGER V. 1966. A radiometric estimate of the duration of sedimentation in the Adelaide Geosyncline, South Australia. *Journal of the Geological Society of Australia* 13, 229-276.

DALY, S. J. & FANNING, C. M. 1993. Archaean. *In:* Drexel, J. F., Preiss, W. V. and
DENTITH M. & MUDGE S. T. 2014 Geophysics for the mineral exploration geoscientist. Cambridge University Press.

FANNING C., FLINT R., PARKER A., LUDWIG K. & BLISSETT A. 1988. Refined Proterozoic evolution of the Gawler craton, South Australia, through U-Pb zircon geochronology. *Precambrian Research* 40, 363-386.

FERRIS G. M., SCHWARZ M. P. & HEITHER P. 2015. The Geological Framework, Distribution and Controls of Fe-Oxide Cu-Au Mineralisation in the Gawler Craton, South Australia: Part I-Geological and Tectonic Framework. *Книга*.

FRASER G., BLEWETT R., REID A., KORSCH R., DUTCH R., NEUMANN N., MEIXNER A., SKIRROW R., COWLEY W. & SZPUNAR M. 2010 Geological interpretation of deep seismic reflection and magnetotelluric line 08GA-G1: Eyre Peninsula, Gawler Craton, South Australia. South Australian seismic and MT workshop. pp. 81-95.

GRAUCH V. S. Geophysical tools for defining covered geologic fea tures: significance for disseminated gold deposits in Nevada, USA. *Bicentennial Gold* 88, 527-529.

INVESTIGATOR RESOURCES LIMITED. 2014. Thurlga Joint Venture with Investigator Resources Limited to explore for new Eyre Peninsula deposits [AVALIBLE ONLINE] [Viewed 31/03/2015] http://www.adelaideresources.com.au/announcements/20140818%20Thurlga%20Joint%20Venture.pdf

INVESTIGATOR RESOURCES LIMITED. 2015. Presentation to Chief Geologist Group [AVALIABLE ONLINE] [VIEWED 01/04/2015] http://www.investres.com.au/_dbase_upl/250315_Presentation_to_Chief_Geologist_Group.pdf

IRVINE R. & SMITH M. 1990. Geophysical exploration for epithermal gold deposits. *Journal of Geochemical Exploration* 36, 375-412.

JOHNS R. & SOLOMON M. 1953. The age of the Gawler Range Porphyry. *Trans. Roy. Soc. S. Aust* 76, 41-44.

JOHNSON I. & FUJITA M. 1985. The Hishikari gold deposit: an airborne EM discovery. *CIM bulletin* 78, 61-66.

JOHNSON J. P. & MCCULLOCH M. T. 1995. Sources of mineralising fluids for the Olympic Dam deposit (South Australia): Sm□ Nd isotopic constraints. *Chemical Geology* 121, 177-199.

LAMONTAGNE M., THOMAS M., SILLIKER J. & JOBIN D. 2011. Detailed gravity survey to help seismic microzonation: Mapping the thickness of unconsolidated deposits in Ottawa, Canada. *Journal of Applied Geophysics* 75, 444-454.

LOCKE C. & DE RONDE C. 1987. Delineation of gold-bearing hydrothermally altered rocks using gravity data—a New Zealand example. *Geoexploration* 24, 471-481.

LUMB J. 1981. Prospecting for geothermal resources. *Geothermal Systems, Principles and Case Histories, J. Wiley & Sons, New York*, 77-108.

MACLEAN W. & KRANIDIOTIS P. 1987. Immobile elements as monitors of mass transfer in hydrothermal alteration; Phelps Dodge massive sulfide deposit, Matagami, Quebec. *Economic Geology* 82, 951-962.

MORELLI C. 1976. Modern standards for gravity surveys. *Geophysical Journal of the Royal Astronomical Society* 45, 199-199.

NETTLETON L. L. 1942. Gravity and magnetic calculations. *Geophysics* 7, 293-310.

PARKER A. 1993. Kimban Orogeny. *In*: Drexel J., F., Preiss W. V. & Parker A. J. eds. The Geology of South Australia, pp. 71 – 81. Geological Survey of South Australia Bulletin **54**.

REPRESAS P., MONTEIRO SANTOS F. A., RIBEIRO J., RIBEIRO J. A., ALMEIDA E. P., GONÇALVES R., MOREIRA M. & MENDES-VICTOR L. A. 2013. Interpretation of gravity data to delineate structural features connected to low-temperature geothermal resources at Northeastern Portugal. *Journal of Applied Geophysics* 92, 30-38.

RICHARDS S. & COLLINS W. 2004. Growth of wedge-shaped plutons at the base of active half-grabens. *Geological Society of America Special Papers* 389, 309-317.

ROY A. 1962. Ambiguity in geophysical interpretation. *Geophysics* 27, 90-99.

South Australian Resources Information Geoserver 2015, SARIG, Available from <sarig.pir.sa.gov.au>. [8th October 2015].

SIBSON R. H. & SCOTT J. 1998. Stress/fault controls on the containment and release of overpressured fluids: Examples from gold-quartz vein systems in Juneau, Alaska; Victoria, Australia and Otago, New Zealand. *Ore Geology Reviews* 13, 293-306.

SIMMONS G. 1964. Gravity survey and geological interpretation, northern New York. *Geological Society of America Bulletin* 75, 81-98.

SKEELS D. C. 1947. Ambiguity in gravity interpretation. *Geophysics* 12, 43-56.

STIERMAN D. J. 1984. Geophysical and geological evidence for fracturing, water circulation and chemical alteration in granitic rocks adjacent to major strike□slip faults. *Journal of Geophysical Research: Solid Earth (1978–2012)* 89, 5849-5857.

THOMSON B. 1970. A review of the Precambrian and Lower Palaeozoic tectonics of South Australia. *Trans. R. Soc. S. Aust* 94, 193-221.

TURNER A.R.1970. Some aspects of the geology of the Gawler Ranges Volcanic Complex, *South Australian Government Department of Mines* 703.

VAJK R. 1956. BOUGUER CORRECTIONS WITH VARYING SURFACE DENSITY. *GEOPHYSICS* 21, 1004-1020.

VASSALLO J. & WILSON J. 2001. Structural repetition of the Hutchison Group metasediments, Eyre Peninsula, South Australia. *Australian Journal of Earth Sciences* 48, 331-345.

WEBB A., THOMSON B., BLISSETT A., DALY S., FLINT R. & PARKER A. 1986. Geochronology of the Gawler Craton, South Australia. *Australian Journal of Earth Sciences* 33, 119-143.

WHITTEN E. T. 1963. Application of quantitative methods in the geochemical study of granitic massifs. *Roy. Soc. Canada Sp. Publ.* 6, 75-123.

WIEBE R. & COLLINS W. 1998. Depositional features and stratigraphic sections in granitic plutons: implications for the emplacement and crystallization of granitic magma. *Journal of Structural Geology* 20, 1273-1289.

XU C., WANG H.-H., LUO Z.-C., NING J.-S. & LIU H.-L. 2015. Multilayer stress from gravity and its tectonic implications in urban active fault zone: A case study in Shenzhen, South China. *Journal of Applied Geophysics* 114, 174-182.

YONG-XIONG Y. 1994. A RESEARCH ON THE CONVERSION OF GRAVITY FIELD INTO REGIONAL TECTONIC STRESS FIELD. *Chinese Journal of Geophysics*, p.S2.

ZHDANOV M. S. 2002 Geophysical inverse theory and regularization problems. Elsevier.

APPENDIX A: BUCKLEBOO LINE AND SIAM LINE RAW DATA

The following is the raw spread sheet data for both the Buckleboo and Siam line.

Obs_g_1965_mgals	Longitude_GDA94	Latitude_GDA94	Easting_GDA94	Northing_GDA94
979508.6323	136.6611665	-32.7529149	655619.4557	6374883.6
979507.9579	136.6659465	-32.74318804	656084.2655	6375955.
979507.9818	136.6712287	-32.73626739	656591.3268	6376714.
979508.8669	136.6729145	-32.72693638	656765.6408	6377746.7
979507.3192	136.6762741	-32.71871013	657094.9287	6378653.8
979506.4207	136.678693	-32.70971318	657337.4512	6379647.
979505.176	136.6813859	-32.70115724	657604.9212	6380592.4
979505.0318	136.6811108	-32.69175642	657595.6583	6381635.1
979503.6521	136.6857205	-32.6837565	658041.9426	6382515.2
979499.1203	136.6903827	-32.67556455	658493.5642	6383416.6
979495.2597	136.6952048	-32.66708514	658960.7724	6384349.5
979493.1164	136.6931154	-32.66389742	658770.4613	6384706.1
979494.0827	136.7007752	-32.65019367	659513.1858	6386214.0
979494.6666	136.6916227	-32.64239416	658668.4569	6387092.4
979496.7441	136.6956506	-32.63318504	659062.6073	6388107.5
979497.1951	136.7038112	-32.62457779	659843.5298	6389049.5
979496.2296	136.708002	-32.61936588	660246.0234	6389621.1
979493.5764	136.714038	-32.61205554	660825.4742	6390422.5
979492.711	136.7195234	-32.60516612	661352.5805	6391178.0
979494.8016	136.7269921	-32.59780677	662066.7545	6391982.6
979495.3347	136.7286222	-32.59562539	662223.6817	6392222.
979495.3065	136.7295574	-32.59323806	662315.7671	6392485.3
979495.7205	136.7305671	-32.59133992	662413.9612	6392694.2
979495.2761	136.7320126	-32.58968986	662552.6133	6392874.9
979494.8989	136.7335464	-32.58769652	662700.1863	6393093.6
979494.5736	136.7352267	-32.5855068	662861.8682	6393333.8
979494.2774	136.736509	-32.58384293	662985.2509	6393516.
979494.0372	136.737917	-32.5820133	663120.7404	6393717.
979493.3247	136.7391753	-32.58036986	663241.8371	6393897.3
979493.1986	136.7405575	-32.57856869	663374.8523	6394094.9
979493.0042	136.7418065	-32.57682582	663495.268	6394286.2
979492.8911	136.7425231	-32.57651218	663563.1116	6394319.9
979491.5235	136.7519038	-32.57115877	664453.5268	6394899.0
979489.1016	136.7626184	-32.5650242	665470.7212	6395562.5
979487.674	136.7702494	-32.55894046	666198.4251	6396225.2
979488.6043	136.778385	-32.55244242	666974.3644	6396932.9
979491.0412	136.7874646	-32.54692406	667837.2505	6397530.5
979490.9071	136.7854677	-32.53687508	667668.4063	6398647.8
979491.5332	136.7799189	-32.53025211	667159.5321	6399390.8
979491.5301	136.771399	-32.525272	666368.4685	6399956.4
979491.9623	136.7617894	-32.52217389	665471.4949	6400314.8

979483.7659	135.814942	-32.45282512	576596.0205	6409077.945	53	200.3610916	201.446	9794697.989	-11.26573987	9794697.209	-113.4373987	-115.4977477
979484.3161	135.8188127	-32.46012435	576953.6284	6408266.002	53	200.2375086	201.33	9794703.493	-11.33539119	9794702.713	-114.1339119	-116.2070938
979483.1548	135.8211876	-32.47037033	577168.0922	6407128.465	53	208.9312816	210.044	9794691.874	-11.62175985	9794691.094	-116.9975985	-119.2384248
979484.3783	135.8247918	-32.4788303	577499.5488	6406188.017	53	203.159499	204.29	9794704.116	-12.2217851	9794703.336	-122.997851	-125.1883562
979484.4494	135.8266149	-32.48746908	577663.435	6405229.032	53	204.9042857	206.056	9794704.828	-12.51044024	9794704.048	-125.8844024	-128.1421268
979484.9895	135.8291227	-32.49631673	577891.43	6404246.388	53	203.5984477	204.769	9794710.231	-12.94764061	9794709.451	-130.2564061	-132.5316799
979488.6138	135.8352997	-32.50352422	578465.4817	6403442.863	53	188.6203596	189.799	9794746.494	-12.8561273	9794745.714	-129.341273	-131.4106162
979488.6648	135.8358739	-32.50664186	578516.7116	6403096.831	53	188.0298727	189.216	9794747.004	-13.17511098	9794746.224	-132.5311098	-134.6063357
979488.3908	135.8362828	-32.50900697	578553.0707	6402834.342	53	190.3283867	191.521	9794744.262	-13.1895274	9794743.482	-132.675274	-134.7972812
979488.0013	135.8365867	-32.51134033	578579.5869	6402575.45	53	192.7777975	193.977	9794740.365	-13.28726493	9794739.585	-133.6526493	-135.8238497
979488.3324	135.8370729	-32.51292229	578623.8785	6402399.72	53	192.4776151	193.681	9794743.678	-13.14375217	9794742.898	-132.2175217	-134.3924556
979488.6854	135.8377995	-32.51514821	578690.1832	6402152.426	53	191.7916536	193	9794747.21	-13.10680094	9794746.43	-131.8480094	-134.0224733
979488.9904	135.8378701	-32.51775691	578694.5422	6401863.183	53	190.2503639	191.467	9794750.261	-13.31688065	9794749.481	-133.9488065	-136.116675
979488.5032	135.8375093	-32.51958222	578659.0682	6401661.102	53	191.3739458	192.597	9794745.386	-13.73159768	9794744.606	-138.0959768	-140.2930918
979488.585	135.8374719	-32.52190835	578653.5319	6401403.262	53	191.2447778	192.475	9794746.206	-13.86422197	9794745.426	-139.4222197	-141.6314696
979488.3797	135.8372784	-32.52437774	578633.2006	6401129.657	53	191.3981754	192.637	9794744.151	-14.24004404	9794743.371	-143.1804404	-145.408835
979488.2845	135.8372822	-32.5265781	578631.643	6400885.73	53	191.9001536	193.146	9794743.198	-14.41546023	9794742.418	-144.9346023	-147.1841981
979487.935	135.8371637	-32.52833087	578618.9918	6400691.51	53	192.7333832	193.985	9794739.702	-14.74370567	9794738.922	-148.2170567	-150.4903104
979487.8658	135.8369562	-32.53018041	578597.8923	6400486.629	53	193.7204727	194.978	9794739.01	-14.76909017	9794738.23	-148.4709017	-150.7703633
979487.7334	135.8370332	-32.53204132	578603.5037	6400280.278	53	195.2273318	196.491	9794737.685	-14.75642732	9794736.905	-148.3442732	-150.6780748
979487.6061	135.8383941	-32.53433564	578729.2994	6400024.932	53	199.5006493	200.767	9794736.411	-14.23067318	9794735.631	-143.0867318	-145.4889062
979486.8347	135.8398241	-32.53594809	578862.1816	6399845.123	53	204.6010007	205.868	9794728.693	-14.13120237	9794727.913	-142.0920237	-144.5706755
979486.2512	135.8405866	-32.53818539	578931.823	6399596.538	53	208.1163728	209.388	9794722.854	-14.20599393	9794722.074	-142.8399393	-145.3794232
979483.5793	135.8464018	-32.54574481	579471.2336	6398754.198	53	220.5359575	221.815	9794696.122	-15.05429448	9794695.342	-151.3229448	-154.0591404
979487.7219	135.8546686	-32.55396624	580240.1424	6397836.593	53	204.9338326	206.218	9794737.569	-14.65123654	9794736.789	-147.2923654	-149.8089311
979490.722	135.8601968	-32.56110573	580752.7732	6397040.947	53	193.348129	194.645	9794767.586	-14.51108104	9794766.806	-145.8908104	-148.2608718
979493.8259	135.8650397	-32.56905093	581200.2697	6396156.475	53	182.5462425	183.859	9794798.642	-14.1783817	9794797.862	-142.563817	-144.8045171
979496.5921	135.8649212	-32.57838869	581180.7338	6395121.401	53	170.1403349	171.487	9794826.318	-14.60985001	9794825.538	-146.8785001	-149.0007444
979497.9084	135.8649719	-32.58103285	581183.1055	6394828.236	53	166.7476807	168.104	9794839.488	-14.17510966	9794838.708	-142.5310966	-144.6215372
979498.2541	135.8653931	-32.5833449	581220.5508	6394571.606	53	165.6916668	167.054	9794842.948	-14.22526838	9794842.168	-143.0326838	-145.1191583
979498.4471	135.8658703	-32.58549053	581263.4057	6394333.381	53	164.591653	165.961	9794844.879	-14.42308574	9794844.099	-145.0108574	-147.0945951
979499.128	135.866573	-32.58759414	581327.4611	6394099.642	53	163.1676555	164.542	9794851.691	-14.19341195	9794850.911	-142.7141195	-144.7862881
979499.9654	135.8680685	-32.58962426	581465.98	6393873.442	53	161.3934714	162.77	9794860.069	-13.87068555	9794859.289	-139.4868555	-141.5366403
979500.4433	135.8696206	-32.59152447	581609.9217	6393661.597	53	160.0766125	161.455	9794864.851	-13.80699198	9794864.071	-138.8499198	-140.8835254
979500.7532	135.8703133	-32.59350571	581673.1313	6393441.43	53	159.1477055	160.531	9794867.951	-13.84117817	9794867.171	-139.1917817	-141.2210366
979501.0509	135.8710347	-32.59586062	581738.6949	6393179.814	53	157.939651	159.328	9794870.93	-13.9730503	9794870.15	-140.510503	-142.5314907
979501.3589	135.8714498	-32.59855332	581775.2039	6392880.987	53	158.7211117	160.118	9794874.012	-13.73029192	9794873.232	-138.0829192	-140.1323601
979500.2769	135.8715971	-32.59954542	581788.1278	6392770.89	53	160.0624706	161.462	9794863.186	-14.38397199	9794862.406	-144.6197199	-149.1535053
979499.9882	135.8715428	-32.60090727	581781.7919	6392619.96	53	162.4557535	163.86	9794860.298	-14.31283057	9794859.518	-143.9083057	-148.4872713
979500.2168	135.8716565	-32.60190076	581791.5616	6392509.735	53	164.1985561	165.606	9794862.585	-13.82216901	9794861.805	-139.0016901	-143.6130677
979500.6439	135.8708661	-32.60452236	581715.0084	6392219.717	53	163.8608872	165.28	9794866.858	-13.67399054	9794866.078	-137.5199054	-142.1492112
979500.8709	135.8696689	-32.60661726	581600.7677	6391988.398	53	162.7743304	164.204	9794869.129	-13.83036315	9794868.349	-139.0836315	-143.7174536
979501.9542	135.8691689	-32.60925446	581551.4681	6391696.426	53	162.9975306	164.438	9794879.968	-12.91673576	9794879.188	-129.9473576	-134.6057991
979502.4472	135.8695005	-32.61116672	581580.8407	6391484.181	53	161.8495065	163.296	9794884.901	-12.80492526	9794884.121	-128.8292526	-133.4823521
979502.4912	135.8704773	-32.61380384	581670.1012	6391191.083	53	160.7620899	162.214	9794885.34	-13.19012984	9794884.56	-132.6812984	-137.3287638
979505.7042	135.8773635	-32.62113978	582309.4891	6390372.519	53	148.5185042	149.973	9794917.488	-12.98496878	9794916.708	-130.6296878	-135.0981785
979506.4734	135.8816292	-32.63009936	582701.4459	6389375.956	53	147.6475536	149.12	9794925.184	-13.11826584	9794924.404	-131.9626584	-136.4533762
979506.0831	135.8770036	-32.63783608	582260.4445	6388521.861	53	148.0786301	149.593	9794921.279	-14.05057466	9794920.499	-141.2857466	-145.8655371
979506.7873	135.8781838	-32.64770922	582362.0991	6387426.418	53	147.3611912	148.904	9794928.324	-14.29185694	9794927.544	-143.6985694	-148.323564
979505.4427	135.8747336	-32.6565043	582030.4695	6386454.072	53	155.4670656	157.051	9794914.871	-14.75656711	9794914.091	-148.3456711	-153.1737062
979504.2441	135.8775124	-32.66514028	582283.1527	6385494.541	53	165.0150281	166.618	9794902.879	-14.78288232	9794902.099	-148.6088232	-153.6176372
979501.0668	135.8823766	-32.67294327	582732.0918	6384625.722	53	182.3582255	183.971	9794871.09	-15.18917512	9794870.31	-152.6717512	-157.9588101
979505.1333	135.8886545	-32.68031103	583313.8846	6383804.021	53	160.6386925	162.255	9794911.775	-15.99714259	9794910.995	-160.7514259	-165.7209227
979508.7155	135.8958788	-32.68799369	583984.0161	6382946.624	53	148.1894185	149.806	9794947.616	-15.49269864	9794946.836	-155.7069864	-160.4897959
979507.704	135.9047222	-32.69234756	584808.9566	6382456.916	53	146.5780308	148.178	9794937.496	-17.18255774	9794936.716	-172.6055774	-177.3313731
979509.0174	135.9129424	-32.69772848	585574.4149	6381853.782	53	145.9068718	147.495	9794950.637	-16.44481297	9794949.857	-165.2281297	-169.9204855
979507.6948	135.9207813	-32.70394963	586303.229	6381157.747	53	148.974133	150.553	9794937.404	-17.67764006	9794936.624	-177.5564006	-182.2767861
979507.3205	135.9279068	-32.71106314	586964.2111	6380363.314	53	150.6960044	152.271	9794933.659	-18.29858929	9794932.879	-183.7658929	-188.5046127
979506.6341	135.937755	-32.71586076	587882.5206	6379823.323	53	157.4284452	158.98	9794926.792	-18.05985767	9794926.012	-181.3785767	-186.1724327
979504.5062	135.9421851	-32.72396885	588289.7125	6378920.766	53	167.0429059	168.6	9794905.502	-18.96288595	9794904.722	-190.4088595	-195.3578533
979503.0956	135.9509605	-32.72993346	589106.1319	6378252.174	53	174.4968368	176.037	9794891.388	-19.40159435	9794890.608	-194.7959435	-199.8230576
979502.1261	135.9605337	-32.73332878	589999.7732	6377867.672	53	181.3963136	182.909	9794881.688	-19.29894671	9794880.908	-193.7694671	-198.8453558
979504.4088	135.9706098	-32.73581467	590941.3929	6377583.477	53	171.4745543	172.957	9794904.527	-19.17690515	9794903.747	-192.5490515	-197.4173832
979505.7462	135.9818001	-32.7375547	591988.1272	6377380.912	53	168.1782103	169.625	9794917.908	-18.63724404	9794917.128	-187.1524404	-191.9012581
979504.6187	135.9920852	-32.74050409	592948.7534	6377044.957	53	172.1288437	173.545	9794906.627	-19.23674854	9794905.847	-193.1474854	-197.895068
979502.9619	136.0022277	-32.74416356	593895.2071	6376630.313	53	177.7273407	179.116	9794890.051	-20.09936983	9794889.271	-201.7736983	-206.5507167
979501.3542	136.0123669	-32.74619811	594842.9962	6376395.723	53	182.1450141	183.504	9794873.965	-21.01206181	9794873.185	-210.9006181	-215.6850224
979499.3984	136.0199355	-32.75176388	595546.1441	6375771.881	53	187.8596245	189.206	9794854.396	-22.30492516	9794853.616	-223.8292516	-228.6738291
979498.659	136.0261805	-32.7584095	596124.0504	6375029.475	53	194.5681097	195.908	9794846.999	-22.27279392	9794846.219	-223.5079392	-228.4393101
979497.5335	136.0344183	-32.76412719	596889.5435	6374388.084	53	204.5865006	205.91	9794835.737	-21.90169153	9794834.957	-219.7969153	-224.8442
979495.2865	136.0454974	-32.76532118	597926.0217	6374245.518	53	213.4362164	214.722	9794813.256	-22.51470988	9794812.476	-225.9270988	-231.0305128
979493.4577	136.0543674	-32.77162341	598749.8985	6373538.588	53	224.6791346	225.948	9794794.958	-22.65460147	9794794.178	-227.3260147	-232.5611823
979487.2173	136.0564045	-32.77996295	598931.4666	6372612.131	53	248.282014	249.562	9794732.521	-24.93934653	9794731.741	-250.1734653	-255.7747209
979486.9541	136.0627939	-32.78775423	599521.1812	6371742.365	53	253.1194617	254.394	9794729.887	-24.89313042	9794729.107	-249.7113042	-255.3720519
979485.1833	136.0700115	-32.79483876	600189.1396	6370950.129	53	263.2168271	264.482	9794712.17	-25.26334678	9794711.39	-253.4134678	-259.2018225
979482.1519	136.0697823	-32.79980845	600162.1002	6370399.384	53	282.8171286	284.094	9794681.84	-24.84752583	9794681.06	-249.2552583	-255.3484144
979481.0482	136.0681774	-32.80349217	600007.7053	6369992.509	53	288.7529691	290.043	9794670.798	-25.08469456	9794670.018	-251.6269456	-257.8309512
979485.5725	136.0682911	-32.81280069	600007.9214	6368960.415	53	270.8021678	272.112	9794716.065	-24.85100102	9794715.285	-249.2900102	-255.2758225
979487.4195	136.0685219	-32.81582771	600026.1371	6368624.606	53	262.7102613	264.026	9794734.544	-24.84267454	9794733.764	-249.2067454	-255.0876305
979488.0054	136.0695955	-32.81787157	600124.3515	6368396.998	53	263.5722934	264.889	9794740.406	-24.25492666	9794739.626	-243.3292666	-249.2245207
979488.2128	136.0707169	-32.81984277	600227.115	6368177.398	53	263.7061915	265.023	9794742.481	-24.1833362	9794741.701	-242.613362	-248.5107729
979489.4558	136.0707246	-32.82217029	600225.2236	6367919.35	53	258.5867544	259.909	9794754.917	-24.1371702	9794754.137	-242.151702	-247.9859156
979490.0793	136.0700419	-32.82489986	600158.2502	6367617.384	53	257.1162031	258.447	9794761.156	-24.02553286	9794760.376	-241.0353286	-246.8651503
979491.4761	136.0695868	-32.82706956	600113.2205	6367377.271	53	252.9081565	254.245	9794775.132	-23.63309053	9794774.352	-237.1109053	-242.8917422
979491.7905	136.0692939	-32.82918477	600083.4296	6367143.045	53	250.1780292	251.521	9794778.277	-24.02848729	9794777.497	-241.0648729	-246.8182221
979493.6906	136.0691508	-32.83188337	600067.007	6366844.001	53	244.8586969	246.208	9794797.288	-23.3946384	9794796.508	-234.726384	-240.4149987
979495.7707	136.0702607	-32.83429992	600168.1773	6366575.037	53	238.9844565	240.335	9794818.1	-22.66752779	9794817.32	-227.4552779	-233.0608802
979496.5343	136.0713508	-32.83646596	600267.7777	6366333.865	53	237.8820105	239.233	9794825.74	-22.29860379	9794824.96	-223.7660379	-229.3564771
979497.512	136.0723644	-32.83838995	600360.4811	6366119.599	53	238.6383393	239.99	9794835.522	-21.32992496	9794834.742	-214.0792496	-219.6820524
979498.5166	136.0732195	-32.84042611	600438.2113	6365893.046	53	235.5766105	236.93	9794845.574	-21.09427428	9794844.794	-211.7227428	-217.2843313
979500.1965	136.073346	-32.84258837	600447.6172	6365653.207	53	230.4145962	231.772	9794862.382	-20.60608908	9794861.602	-206.8408908	-212.335025
979502.1165	136.0734756	-32.84477606	600457.2868	6365410.544	53	225.8907234	227.252	9794881.592	-19.75428447	9794880.812	-198.3228447	-203.7584395
979504.3556	136.073405	-32.84697538	600448.1957	6365166.783	53	219.6610727	221.026	9794903.994	-18.9197921	9794903.214	-189.977921	-195.3293913
979505.2493	136.0732962	-32.8486371	600436.1433	6364982.659	53	215.8662067	217.235	9794912.936	-18.90814459	9794912.156	-189.8614459	-195.1647967
979506.7042	136.0787412	-32.85654111	600936.7462	6364101.185	53	209.9827214	211.348	9794927.493	-19.26131625	9794926.713	-193.3931625	-198.6030666
979509.0403	136.0842323	-32.86444561	601441.5695	6363219.583	53	206.1443134	207.505	9794950.867	-18.33082704	9794950.087	-184.0882704	-189.2325978
979506.7559	136.0895476	-32.87207678	601930.1677	6362368.425	53	221.1498814	222.506	9794928.01	-18.29432984	9794927.23	-183.7232984	-189.0795137
979505.2817	136.0947532	-32.87954949	602408.5978	6361534.914	53	232.0693562	233.421	9794913.26	-18.23790212	9794912.48	-183.1590212	-188.6663841
979502.1998	136.1001719	-32.88734409	602906.4993	6360665.482	53	249.2722901	250.619	9794882.426	-18.58071879	9794881.646	-186.5871879	-192.3354399

Buckleboo

Northing_GDA94	BA_1984_mgals
6409786	-10.771
6409078	-11.2657
6408266	-11.3354
6407128	-11.6218
6406188	-12.2218
6405229	-12.5104
6404246	-12.9476
6403443	-12.8561
6403097	-13.1751
6402834	-13.1895
6402575	-13.2873
6402400	-13.1438
6402152	-13.1068
6401863	-13.3169
6401661	-13.7316
6401403	-13.8642
6401130	-14.24
6400886	-14.4155
6400692	-14.7437
6400487	-14.7691
6400280	-14.7564
6400025	-14.2307
6399845	-14.1312
6399597	-14.206
6398754	-15.0543
6397837	-14.6512
6397041	-14.5111
6396156	-14.1784
6395121	-14.6099
6394828	-14.1751
6394572	-14.2253
6394333	-14.4231
6394100	-14.1934
6393873	-13.8707
6393662	-13.807
6393441	-13.8412
6393180	-13.9731
6392881	-13.7303
6392771	-14.384
6392620	-14.3128
6392510	-13.8222

6392220	-13.674
6391988	-13.8304
6391696	-12.9167
6391484	-12.8049
6391191	-13.1901
6390373	-12.985
6389376	-13.1183
6388522	-14.0506
6387426	-14.2919
6386454	-14.7566
6385495	-14.7829
6384626	-15.1892
6383804	-15.9971
6382947	-15.4927
6382457	-17.1826
6381854	-16.4448
6381158	-17.6776
6380363	-18.2986
6379823	-18.0599
6378921	-18.9629
6378252	-19.4016
6377868	-19.2989
6377583	-19.1769
6377381	-18.6372
6377045	-19.2367
6376630	-20.0994
6376396	-21.0121
6375772	-22.3049
6375029	-22.2728
6374388	-21.9017
6374246	-22.5147
6373539	-22.6546
6372612	-24.9393
6371742	-24.8931
6370950	-25.2633
6370399	-24.8475
6369993	-25.0847
6368960	-24.851
6368625	-24.8427
6368397	-24.2549
6368177	-24.1833
6367919	-24.1372
6367617	-24.0255
6367377	-23.6331

6367143	-24.0285
6366844	-23.3946
6366575	-22.6675
6366334	-22.2986
6366120	-21.3299
6365893	-21.0943
6365653	-20.6061
6365411	-19.7543
6365167	-18.9198
6364983	-18.9081
6364101	-19.2613
6363220	-18.3308
6362368	-18.2943
6361535	-18.2379
6360665	-18.5807
6359734	-18.7425
6358849	-19.0266

Siam

Northing_GDA94	BA_1984_mgals
6374884	-7.81124
6375955	-6.13067
6376715	-5.43429
6377747	-5.20566
6378654	-6.39667
6379648	-4.85595
6380592	-5.84476
6381635	-5.83823
6382515	-6.74023
6383417	-8.21497
6384350	-8.85205
6384706	-8.75771
6386214	-11.2977
6387092	-11.5039
6388108	-12.7438
6389050	-13.1138
6389621	-13.1325
6390423	-14.4228
6391178	-14.2351
6391983	-14.0688
6392222	-13.8927
6392485	-14.0081

6392694	-13.9653
6392875	-14.425
6393094	-14.7002
6393334	-14.7529
6393516	-14.6544
6393717	-14.418
6393897	-14.771
6394095	-14.811
6394286	-15.284
6394320	-15.3173
6394899	-15.4389
6395563	-15.6325
6396225	-15.0726
6396933	-14.9586
6397531	-14.3376
6398648	-15.0322
6399391	-14.2492
6399956	-14.6535
6400315	-14.8263
6401081	-14.311